



Delft University of Technology

An inter-city energy migration framework for regional energy balance through daily commuting fuel-cell vehicles

He, Yingdong; Zhou, Yuekuan; Liu, Jia; Liu, Zhengxuan; Zhang, Guoqiang

DOI

[10.1016/j.apenergy.2022.119714](https://doi.org/10.1016/j.apenergy.2022.119714)

Publication date

2022

Document Version

Final published version

Published in

Applied Energy

Citation (APA)

He, Y., Zhou, Y., Liu, J., Liu, Z., & Zhang, G. (2022). An inter-city energy migration framework for regional energy balance through daily commuting fuel-cell vehicles. *Applied Energy*, 324, Article 119714. <https://doi.org/10.1016/j.apenergy.2022.119714>

Important note

To cite this publication, please use the final published version (if applicable). Please check the document version above.

Copyright

Other than for strictly personal use, it is not permitted to download, forward or distribute the text or part of it, without the consent of the author(s) and/or copyright holder(s), unless the work is under an open content license such as Creative Commons.

Takedown policy

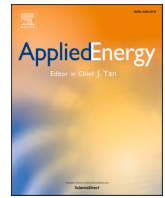
Please contact us and provide details if you believe this document breaches copyrights. We will remove access to the work immediately and investigate your claim.

Green Open Access added to TU Delft Institutional Repository

'You share, we take care!' - Taverne project

<https://www.openaccess.nl/en/you-share-we-take-care>

Otherwise as indicated in the copyright section: the publisher is the copyright holder of this work and the author uses the Dutch legislation to make this work public.



An inter-city energy migration framework for regional energy balance through daily commuting fuel-cell vehicles

Yingdong He^{a,d}, Yuekuan Zhou^{b,c,e,*}, Jia Liu^{f,g,h}, Zhengxuan Liu^{a,i}, Guoqiang Zhang^a

^a College of Civil Engineering, National Center for International Research Collaboration in Building Safety and Environment, Hunan University, Changsha, Hunan, China

^b Sustainable Energy and Environment Thrust, Function Hub, The Hong Kong University of Science and Technology (Guangzhou), Nansha, Guangzhou 511400, Guangdong, China

^c HKUST Shenzhen-Hong Kong Collaborative Innovation Research Institute, Futian, Shenzhen, China

^d Center for the Built Environment, University of California, Berkeley, CA, USA

^e Department of Mechanical and Aerospace Engineering, The Hong Kong University of Science and Technology, Clear Water Bay, Hong Kong Special Administrative Region

^f School of Civil Engineering, Guangzhou University, Guangzhou, China

^g Department of Building Environment and Energy Engineering, Faculty of Construction and Environment, Hong Kong Polytechnic University, Kowloon, Hong Kong, China

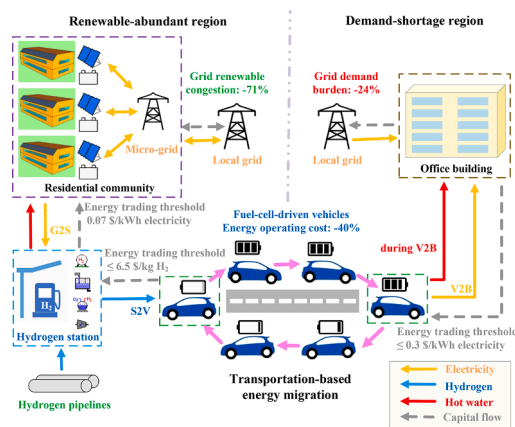
^h Guangdong Provincial Key Laboratory of Building Energy Efficiency and Application Technologies, Guangzhou University, Guangzhou, China

ⁱ Faculty of Architecture and The Built Environment, Delft University of Technology, Delft, The Netherlands

HIGHLIGHTS

- An inter-city energy migration framework for regional renewable energy sharing.
- Multidirectional energy sharing and trading through hydrogen networks.
- Optimal grid-regulation strategies to stabilize grid power and reduce energy costs.
- Critical threshold on energy trading price to encourage participation motivation.
- Carbon-neutrality transition in regional districts with hydrogen energy.

GRAPHICAL ABSTRACT



ARTICLE INFO

Keywords:

Transportation-based Inter-city energy migration
Spatiotemporal energy sharing network
Innovative Grid-regulation strategy
Distributed hydrogen infrastructure

ABSTRACT

Spatiotemporal energy interaction and sharing are promising solutions to penetrate renewable energy, enhance grid power stability, and improve regional energy flexibility. However, the current literature is restrained in a small-scale neighborhood level, without considering inter-city energy migration through spatiotemporal complementarity between renewable-abundant regions (like suburb or countryside areas) and demand-shortage regions (like city centers). In this study, the energy interaction boundary is extended from a neighborhood scale

* Corresponding author at: Sustainable Energy and Environment Thrust, Function Hub, The Hong Kong University of Science and Technology (Guangzhou), Nansha, Guangzhou 511400, Guangdong, China.

E-mail addresses: yuekuanzhou@ust.hk, yuekuan.zhou@connect.polyu.hk (Y. Zhou).

<https://doi.org/10.1016/j.apenergy.2022.119714>

Received 8 November 2021; Received in revised form 21 June 2022; Accepted 17 July 2022

Available online 31 July 2022

0306-2619/© 2022 Elsevier Ltd. All rights reserved.

Energy trading
Hydrogen economy

to an inter-city scale, to maximize the renewable energy penetration, demand coverage, and reduce regional energy imbalance. This study firstly proposes a holistic framework on inter-city transportation-based energy migration, consisting of a residential community with rooftop photovoltaic systems and electrical batteries, an office building, hydrogen vehicles (HVs), a hydrogen (H₂) station, and local power grids, for the energy transmission between building groups in spatially different regions through the daily commuting of HVs. Optimal grid-regulation strategies are thereafter proposed and adopted to stabilize the grid power and reduce energy costs. Parametric analysis on energy trading strategies and prices has been conducted, to improve the participation motivations of different stakeholders. Results indicate that, compared to the reference case with isolated buildings and vehicles, the transportation-based energy migration framework covers 23.2 % of the office energy demand and elevates the community's renewable self-use ratio from 72.7 % to 98.6 %. Meanwhile, the maximum grid-export power in the renewable-abundant region (suburb residential community) and the annual grid-import power in the demand-shortage region (city-center office) are reduced by up to 86.9 % (from 155.7 to 20.4 kW) and 29.4 % (from 49.0 to 34.6 kW), respectively. Moreover, even considering the fuel cell degradation cost of HVs, the transportation-based energy migration framework reduces the operating costs of the office building and HVs (the H₂ cost and the fuel cell degradation cost) by 16.4 % (from \$52791.3 to \$44154.7) and 1.7 % (from \$27172.5 to \$26707.4), respectively. Afterward, compared to the reference case, the peak-shaving and load-shaping grid-regulation strategies can decrease the peak grid-export power of the community by about 71.6 % (from 155.7 to 44.2 kW), and the maximum grid-import power of the office by 23.7 % (from 49.0 to 37.4 kW), respectively. Furthermore, the transportation-based energy migration framework is economically feasible, only when the renewable export price for H₂ production is 0.07 \$/kWh, the onsite-renewable-generated H₂ lower than 6.5 \$/kg for the HV owners, and the vehicle-to-building electricity lower than 0.3 \$/kWh for the office building. This study provides a novel inter-city energy migration framework with hydrogen networks to enhance district energy sharing, improve regional energy balance and reduce carbon emission, together with frontier guidelines on energy trading prices to promote participation motivations from different stakeholders.

Nomenclature

Subscription

com	compressor
e, com	community energy demand
ely	electrolyzer
REe, com	renewable energy of the community
surp1, com	surplus renewable energy in the community
short1, com	demand shortage in the community

Abbreviation

C	cost
D	degradation
EC	electricity compensation
exp	export

G2S	micro-grid to the H ₂ station
G2B	grid-to-building
HVAC	Heating, ventilation and air conditioning
HV	Hydrogen vehicle
IC	import cost
imp	import
PEMFC	proton exchange membrane fuel cell
PV	photovoltaic
S2V	H ₂ -station-to-vehicle
SOC	State of charge
SSR	self-sufficiency ratio
SUR	renewable self-use ratio
V2B	vehicle-to-building

1. Introduction

1.1. Background

Buildings, transportation, and industries are three main sectors of energy consumption in human society. Building and transportation sectors now consume more than 60 % of the total energy consumption in the United States of America (U.S.A.) [1] and Europe [2]. The proportion is expected to show a continuous increasing tendency in the upcoming years, especially due to the increased living requirement in buildings (such as cooling [3] and heating [4]) and daily traveling activities. It can be foreseen that buildings and vehicles will impose an increasing burden on power grids and petrol stations in the near future, which brings considerable challenges to the carbon neutralization procedure of the whole society.

In recent years, to reduce the reliance on limited and environment-polluted conventional fossil fuels, electrification and hydrogenation in automobile industry are under fast development, and multiple commercial vehicles equipped with electrochemical batteries or proton exchange membrane fuel cells (PEMFCs) have rapidly developed, e.g., electric-battery vehicles (EVs) like Tesla Model S [5] and hydrogen-

fuel-cell-driven vehicles (HVs) like Toyota Mirai [6]. These new-energy vehicles are powered by electricity or hydrogen (H₂) gas, which can be generated by renewable energy sources, like photovoltaic (PV) systems and wind turbines, and thus actualize zero-carbon emission and environmental-friendliness. Moreover, due to the characteristic of spatial mobility on vehicles, renewable electricity-based or H₂ gas-based sharing networks can be formulated, through the integration of EVs and HVs with buildings. Compared to the case where buildings and vehicles are isolated, integrating buildings and vehicles can reduce the grid dependence and reliance on traditional fossil fuels with increased renewable penetration, and thus strengthen regional energy flexibility and promote decarbonization.

Integrating plug-in vehicles in building energy systems have attracted increasing attention worldwide. Zhou et al. [7] provide a comprehensive review on energy interaction between different types of buildings and vehicles. The review identified technical challenges and provided clear research roadmaps in the research field. The energy sharing network in [8] can reduce the CO₂ emissions and import cost. However, the energy sharing with battery-based vehicles will accelerate the battery cycling aging, due to the increased charging/discharging cycles. Zhou et al. [9] developed an interpretable battery cycling aging model and implemented it in the building-vehicle energy sharing network. The research highlights the necessity for a battery-protective

control strategy. From the lifecycle perspective, the ignorance of battery cycling aging will overestimate economic performance [10]. In addition to electricity-based networks, the hydrogen-based energy sharing network has also been studied. Qian et al. [11] simulated an integrated building-HV system. The renewable energy shared by HVs from the H₂ station to the commercial building can shave 50 % of the peak power from the grid. He et al. [12] proposed a H₂ energy network, integrating a residential community, PV panels, HVs, and a H₂ station installed with an electrolyzer and a compressor, where the onsite-renewable-driven H₂ is produced and stored. The findings indicate that compared to the reference case without energy interaction, integrating buildings and HVs reduce the grid burden by 24.2 % and the annual household energy cost by 38.9 %. Furthermore, by developing a dynamic fuel cell degradation model, He et al. [13] indicated that, the total operating cost might be underestimated by up to 33.4 %, if ignoring the fuel cell degradation. Alavi et al. [14] indicated that the peak grid-import power was reduced by more than 50 % compared to the case when the HVs were not integrated in the energy network. In the simulation work of Sahu et al. [15], a regional energy network was established, integrating 1000 residential houses with PV systems, 500 EVs, and 500 HVs. It was found that the demand coverage ratio was up to 80 %, when the EVs and HVs were used as extended energy storages for the regional energy network. Similar results can also be found in [16].

1.2. The concept of transportation-based energy migration framework

According to the literature review above, one of the key components in building-vehicle energy interactions is the energy storage of vehicles (whether in the form of electricity or H₂), which enlarges the energy storage capacity for enhancing building energy flexibility. Nonetheless, since different regions have various energy production and demand profiles, neighborhood-scale net-zero building-vehicle systems might be only achieved in regions with low energy demands [17] or large spaces for installing complicated renewable systems [18]. When building-vehicle energy networks are extended from a neighborhood scale to a city scale, EVs and HVs might actualize inter-city spatiotemporal energy complementarity between renewable-abundant regions and demand-shortage regions with the daily commuting of vehicles. An analogy

between ants' food-collection circles and transportation-based energy migration framework can help understand how EVs and HVs can reduce regional energy imbalance (Fig. 1):

- (1) When wandering ants find a food source, such as a large piece of bread, each of them carries a small part of the food and takes it back to their nest, where the food is consumed for supporting the activities of the whole ant tribe. Then the empty-handed ants go back to the food source, grab new small parts of the food, and the circle continues.
- (2) In regional energy networks, EVs and HVs act as similar functions as ants in the above-mentioned example. When people commute between different locations, EVs and HVs can be charged in a renewable-abundant region with sufficient renewable energy sources (such as H₂ stations with renewable-produced H₂ gas or countryside buildings with surplus renewable production from rooftop PVs), which are like the food source for the ants. Afterward, EVs and HVs can carry a certain amount of renewable energy and take it to a demand-shortage region such as high-demand office buildings in a city center district, where EVs and HVs are discharged to cover the energy demand of buildings. Thereafter, EVs and HVs may go back to the renewable-abundant region, and continue to carry renewable energy to the demand-shortage region in the next commuting cycle. With the continuous commuting of EVs and HVs between the two regions, a large amount of renewable energy migrates from the renewable-abundant region to the demand-shortage region, enhancing the regional energy balance.

Herein, the concept of transportation-based energy migration is proposed and termed as the energy transmission between buildings or building groups in different regions, through normal transportation activities of EVs or HVs, such as office-home commuting, rather than through specialized energy infrastructures, like power grids, H₂ pipelines, or special trucks, railcars, and ships for H₂ transportation. Compared to conventional energy delivery approaches, like power grids and H₂ pipelines, the transportation-based energy migration framework does not need massive capital investments and infrastructure

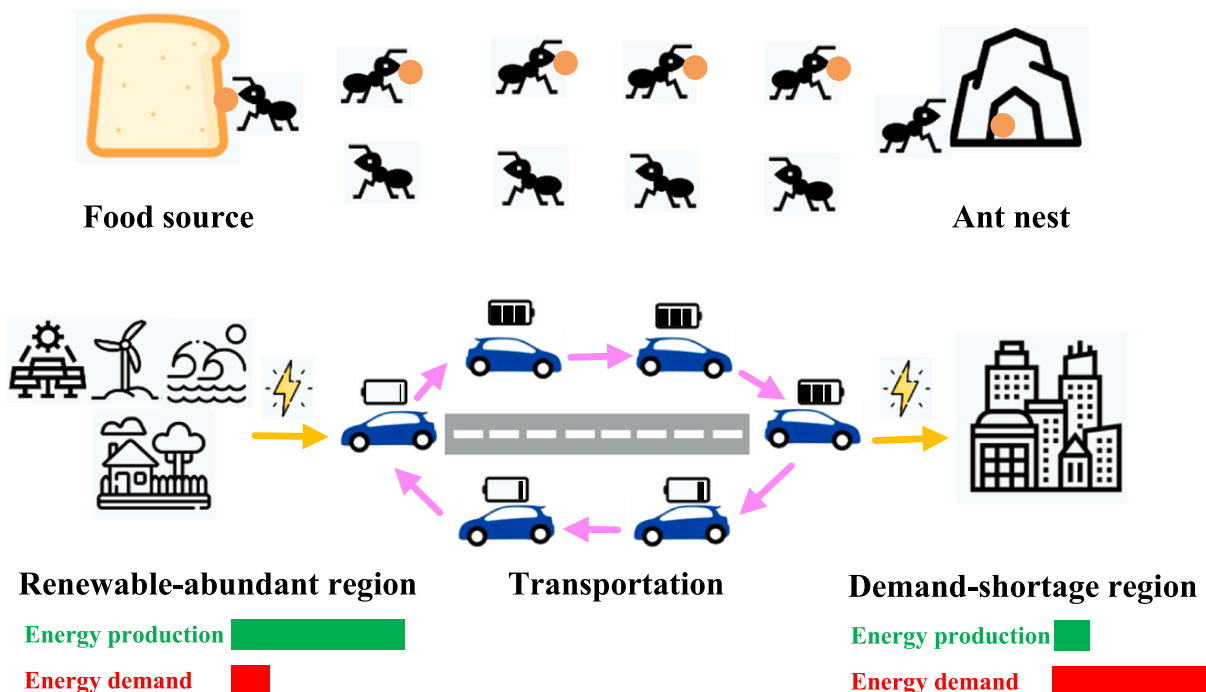


Fig. 1. The analogy between ants' food-collection circles and transportation-based energy migration framework.

construction, and it provides an easy way for normal people (like house owners and vehicle owners) to contribute to regional energy balance and carbon neutralization.

1.3. Scientific gaps

The literature review in Section 1.2 clearly shows the benefits of building-vehicle integrations in terms of energy efficiency, grid stability, and cost savings. Nonetheless, in terms of transportation-based energy migration framework for enhancing regional energy flexibility, some scientific gaps remain unfilled:

- (1) In most previous studies, building-vehicle energy networks are usually restrained within a neighborhood scale. However, considering the almost similar topological structure and energy-use behaviour characteristic, neighborhood energy sharing framework has limited effects on regional energy balance. The idea of transportation-based energy migration framework provides a promising solution to actualize regional energy complementarity between renewable-abundant regions and demand-shortage regions, without massive construction on new energy infrastructures. However, few studies provide a comprehensive evaluation on the technical feasibility and potential benefits of transportation-based energy migration framework, such as energy costs, grid regulation, energy flexibility, and so on.
- (2) In the current academia, the HV model in building-vehicle energy networks was simplified without considering dynamic performance degradation (due to large load changing cycles, start-stop cycles, idling time, and maximum power time), thermodynamics, vehicle thermal environment and etc. Simplifications will lead to the underestimation on PEMFCs' performance and the fuel cell degradation caused by daily transportation and vehicle-to-building (V2B) interaction. The consideration on dynamic fuel cell degradation and its dynamic working environment is quite necessary, for energy efficiency and cost analysis on transportation-based energy migration framework, so as to avoid the underestimation or overestimation on techno-economic-environmental performances.
- (3) Previous studies usually evaluate building-vehicle networks through total energy costs, without considering the cost and the participation willingness of each stakeholder. Furthermore, multidirectional energy trading strategies with economic competitiveness have been rarely studied among different stakeholders. Due to the contradiction between the local and the global optimal solutions, the cost-optimal strategy from a stakeholder might lead to the failure of cost-optimal strategy for other stakeholders. For example, a building owner may only care if the building has stable electricity power and how to reduce the electricity cost, with little concern on whether the power is renewable or not. Actually, in practice, a network is economically attractive and feasible with high participation willingness of stakeholders only when every stakeholder has a lower energy cost than the separate building and vehicle systems. However, in the current academia, this contradiction has not been effectively addressed, whereas ignoring these issues will mislead the economic feasibility analysis results.

The goal of this study is to evaluate the techno-economic feasibility of transportation-based energy migration in building-vehicle energy networks. This study proposes an inter-city energy migration network, integrating a residential community with rooftop PV systems and batteries (located in renewable-abundant countryside or suburb), an office building (located in a demand-shortage city center), HVs, a H₂ station with H₂ pipelines, and local power grids, covering the first scientific gap. The renewable electricity produced by rooftop PV systems is used to power the community and to produce H₂ gas to be stored in the high-

pressure tank in the H₂ station. The HVs are then charged with onsite-renewable-produced H₂ at the H₂ station, used for daily commuting, and discharged at the office building for covering the building demand shortage. Furthermore, a two-space cabin thermal model was adopted to calculate the dynamic working environment of vehicle PEMFCs and HVAC energy consumption of vehicles [13]. Multiple criteria, in terms of energy self-sufficiency, renewable self-use ratio, grid interaction, and energy operating costs, are adopted to evaluate the performances of the proposed inter-city energy migration network with and without deploying transportation-based energy migration framework by HVs, which fills the first scientific gap. Meanwhile, a fuel cell degradation model was adopted to calculate the dynamic performance degradation of fuel cells (filling the second scientific gap). Moreover, two grid-regulation strategies (peak-shaving and load-shaping) are proposed for further lowering energy operating costs. Furthermore, advanced energy trading strategies are proposed to ensure the economic feasibility of the transportation-based energy migration framework, and the corresponding energy trading price thresholds among the stakeholders are explored to provide guidance and attract stakeholders' participation willingness, filling the third scientific gap.

Original contributions can be briefly summarized as follows:

- (1) an inter-city energy migration framework was proposed, formulated and mathematically modelled to achieve regional energy balance between renewable-abundant regions (like suburb residential community) and demand-shortage regions (like city-center office) through daily commuting fuel-cell vehicles;
- (2) qualitative and quantitative analysis on techno-economic performance for fuel-cell vehicles based inter-city energy sharing network with consideration on dynamic aging on fuel cells;
- (3) advanced energy trading strategies are proposed, together with identified energy trading price thresholds, to provide frontier guidelines on participation of vehicle owners and building stakeholders in the inter-city energy migration framework.

2. Methods

2.1. Scenario, location, and climate

As shown in Fig. 2, this study configures a scenario, including an office building, located at the center area (San Francisco City Hall) of San Francisco (37 °N, 122 °W), California, U.S.A., and a residential community (including 20 single houses) near University of California Village (namely, UC Village), located at the north of Berkeley. The distance between the office building and the community is about 20 km, with the San Francisco Bay between them. The office building is located in a demand-shortage region where buildings have high energy demands but very limited distributed renewable systems (such as PV panels), due to the limited land space and high land cost. The office building is equipped with solar thermal collectors for covering space heating and domestic hot water use, but has no other renewable systems. The community is located in a renewable-abundant region with many low-rise houses with rooftop PV panels and electrochemical batteries, and it is also powered by the local power grid. A H₂ station is designed near the community with local H₂ pipelines. It is assumed that every working day, ten HVs commute between the office building and the residential community. The HV owners work near the office building and live near the community, and they charge their HVs at the H₂ station. Due to the sea between Berkeley and San Francisco, transferring H₂ through pipelines or electricity through grids between these two cities is very difficult unless massive investment and construction are deployed to build submarine pipelines and power cables. While the energy transfer between these two cities can be actualized through daily transportation, and no massive construction of energy infrastructures is needed. Moreover, it should be noted that battery-driven vehicles are certainly more efficient in energy conversion than HVs, but they have limited capacities for

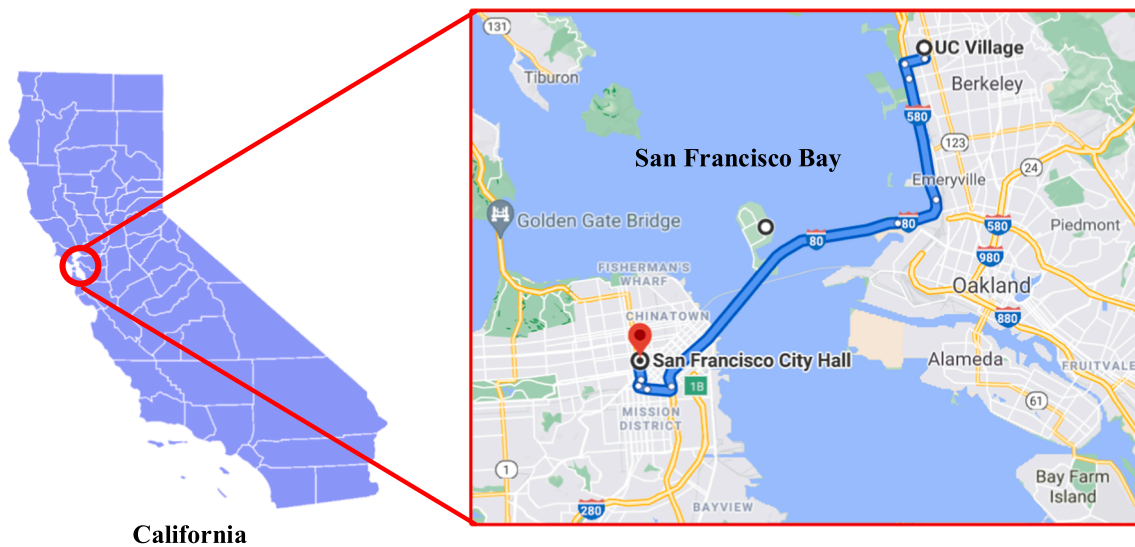


Fig. 2. The location of the proposed scenario (originally from Google Map [19]).

spatial and temporal energy storages: if battery-driven vehicles are used, due to the daily transportation, during the daytime, battery-driven vehicles usually park in San Francisco, and are hard to be charged with the distributed renewable energy of the community; at night when PV panels do not work, vehicles come back and park in the community, and are unable to directly store the onsite renewable electricity. With HVs, the onsite renewable electricity can be converted into H_2 gas and stored in the nearby H_2 station during the daytime; then the onsite-renewable-produced H_2 can be charged to HVs in the evening, and used to cover transportation energy demands or the office building load later during the daytime. Thus, H_2 is more proper for spatial and temporal energy storages than electricity. In terms of local climate, San Francisco is of cool weather with abundant solar energy. The monthly mean outdoor temperature mainly varies between 10 and 16 °C, with the relative humidity at around 70–80 %. Please refer to reference [13] for the detailed climatic parameters.

2.2. Buildings and energy infrastructures

This study adopts the same design of the residential houses (including the rooftop PV systems) and H_2 station, as that of [12], and these two sections shortly describe critical parameters to avoid repetition.

2.2.1. Residential community

The investigated residential community has 60 two-floor houses. The total area of each single house is 400 m² (200 m²/floor), and the heights of the ground and top floors are 3.0 m and 4.5 m, respectively. The houses are divided into three groups with different energy use schedules [12]. To enhance the energy flexibility of the community, electrochemical batteries are deployed in each house with a total capacity at 3000 kWh. These batteries are charged by surplus renewable electricity from the PV systems and are discharged when the community has the demand shortage. As demonstrated in [12], when each house has a total area of 40 m² PV panels, the PV cost is \$11520 for each house, but the PV panels can reduce the electricity cost by more than \$2600 per year, bringing a large economic benefit to the local residents. California also has a Single-Family Affordable Solar Homes (SASH) program and a Multi-family Affordable Solar Homes (MASH) program [20] to cover the PV installation costs of low-income families for enhancing regional energy flexibility and carbon neutralization.

2.2.2. Office building

The office building is located in the center area of San Francisco, and has five floors with a 1000-m² floor area (20 m × 50 m) and a 3-m inner height for each floor.

Building envelope. For each floor of the office building, the areas of north, south, east, and west external windows are 60, 60, 24, and 24 m², respectively, with the total window-wall ratio at 0.4. The configuration of the office building envelope components is shown in Table 1. The thermal insulation of the building envelope complies with the requirements of ASHRAE Standard 90.1 [21].

Occupants. For the office building, each floor has 50 occupants, and the working hours of the office building are 9:00–17:00 during work-days. It is assumed that 30 % of the occupants arrive at the office building at 8:00 and leave at 18:00, while the rest of the occupants only stay in the office building during working hours (9:00–17:00).

Lighting. The largest artificial lighting power of the office building is set at 6 W/m² [22]. It is assumed that the electric power of office equipment is 0.3 W/m² during non-working hours.

Equipment. The largest equipment plug-in power of the office building is set at 7.53 W/m² [21]. It is assumed that the internal heat gain of office equipment during non-working hours is set at 5 % of the largest power (0.38 W/m²).

Rooftop solar thermal collectors. The solar thermal collectors are installed on the rooftop of the office building, with a total collector area

Table 1
Properties of office building envelope.

Envelope	Configuration	Thickness (mm)	U-value (W/m ² K)	SHGC
Wall	10 mm plaster + 300 mm polyurethane + 200 mm wall board + 10 mm wood	520	0.092	–
Ceiling	10 mm timber + 100 mm polyurethane + 150 mm concrete + 10 mm wood	270	0.252	–
Ground floor	10 mm timber + 200 mm polyurethane + 300 mm concrete	510	0.031	–
Roof	10 mm plaster + 300 mm polyurethane + 200 mm wall board + 10 mm wood	520	0.089	–
Window	4 mm glass + 12 mm air gap + 4 mm glass + 12 mm air gap + 4 mm glass	6	0.45	0.37

and tilted angle at 200 m² and 45°. A 20-m³ hot water storage tank is designed for space heating and domestic hot water heating.

Space heating. Space heating mainly relies on the hot water from the solar thermal collectors. The supply hot water temperature is 45 °C for space heating. An auxiliary electric heater is designed to guarantee the supply water temperature at 45 °C. Besides, since the office building usually has high energy loads during the daytime and low loads during the nighttime (which will be clarified in Section 3.2.2) and it has limited renewable energy to cover the loads (as stated in Section 2.1), shifting the building demand to non-peak hours should be considered before expanding the grid capacity. To shift the power from peak period (working hours) to off-peak period (non-working hours), an electric heater is designed to charge the hot water tank at night with a power of 30 kW and a setpoint temperature at 60 °C.

Domestic hot water. The domestic hot water is also mainly produced by the above-mentioned solar thermal collectors, with a daily hot water consumption at 0.022 m³/person [23]. The supplied domestic hot water is also set at 49 °C [24]. If the tank water temperature is not high enough, an electric heater is run to increase the water temperature to 49 °C.

Heat recovery from vehicle PEMFC. Moreover, during the V2B interaction process, a two-stage heat recovery system [13] with non-contact heat transfer between cooling water and vehicle fuel cell coolant is designed to recover the heat from the vehicle PEMFC, so as to pre-heat tap water and save the energy consumption for domestic hot water heating. Specifically, in the first-stage cooling, the vehicle PEMFCs are cooled by a closed-loop with coolant; after absorbing the heat from the PEMFCs, the coolant is cooled by a non-mixed heat exchanger with normal water in the second-stage cooling. This heat recovery system can be established through the integration with the original energy management system of the vehicle PEMFCs (which regulates the running temperature of PEMFCs) via adding a non-mixed heat exchanger on the coolant pipes of the energy management system.

Space cooling. Space cooling is actualized by an air-source chiller (maximum cooling capacity at 300 kW) with the supply cooling water temperature at 7 °C. A 20-m³ water tank is designed to store cold water to avoid the frequent start and stop of the chiller.

Ventilation. The air change rate (ACR) of the office building is set at 2 h⁻¹ during the space heating period, but increases to 3 h⁻¹ during the rest months of a year, to dissipate indoor heat gain. The ACR values are based on ASHRAE Standard 62.1–2019 [25].

All key parameters of the above-mentioned energy components are shown in Section 2.6.

2.2.3. H₂ station

The community is integrated with the H₂ station through the micro-grid, which exports the renewable electricity from the community to the H₂ station for H₂ production. The H₂ station is installed with a 400-kW electrolyzer to absorb the high surplus renewable power during the daytime and a compressor to elevate the onsite-renewable-generated H₂ to 700 bar. The electrolyzer has an idling power of 80 kW, reaching 20 % of the maximum power (corresponding to the realistic idling mode of electrolyzers in practice, which are 10–30 % of the maximum power to start the electrification reactions and ensure the safe running [26]), which means that the electrolyzer can be activated, only when the input electric power is higher than 80 kW. The H₂ station is designed with a storage capacity of 500 kg for storing the onsite-renewable-produced H₂. Besides, a 6-m³ water tank is designed to store the recovered heat during the H₂ production process, which is then sent to the community to cover the domestic hot water heating load. As demonstrated in [12], the electricity-H₂ conversion efficiency is about 64 % (in electrical terms, the usable energy density of hydrogen is 33.3 kWh/kg). With the heat recovery, the energy efficiency is about 70.0 % (the ratio of H₂ energy and recovered heat energy to the renewable energy for H₂ production). Parameters of H₂ system and the heat-recovered water tank are listed in Section 2.6. Furthermore, the current commercial H₂ price from local H₂

pipelines is 16.51 \$/kg for charging HVs [27]. To promote the HV owners to participate in the transportation-based energy migration framework, if V2B interactions are deployed, the onsite-renewable-produced H₂ price is set at 4 \$/kg, corresponding to the fact that the onsite-renewable-produced H₂ is generated using the renewable electricity from the community and the cost of H₂ generated by onsite renewable energy can be 4 \$/kg or even lower [28].

2.2.4. Local grid

The Time-of-Use Plan (E-Tou-D) of the PG&E company [29] is adopted for calculating the grid cost of the residential community (see Table 2). The community also participates in the solar energy project of PG&E, which compensates the grid-import cost by exporting renewable energy to the local grid [30]. Note that, when annual grid-exported electricity is lower than the annual grid-imported electricity, the compensation price of the grid-exported electricity is the same as the grid-imported electricity price, as listed in Table 2. When the annual amount of the community's annual grid-exported electricity surpasses the annual amount of the grid-imported electricity, the surplus renewable energy will be paid by the local government, with the price at \$0.03 per kWh [31]. This study adopts the A-10 Plan of PG&E [29] for calculating the grid cost of the office building. Note that, in terms of calculation on the grid cost, this plan simultaneously considers both the monthly maximum grid-import power and the amount of grid-imported electricity.

2.3. Hydrogen-related vehicle parameters

A HV model is based on a commercial product “Toyota Mirai 2016” [6]. Each Toyota Mirai vehicle provides a 5 kg H₂ tank, with a maximum pressure of 700 bar, a 502 km cruise range, and a maximum power of 114 kW. The H₂ consumption rate of each HV is 0.00996 kg/km for transportation. During weekdays, the HVs depart from the residential community at 7:30, arrive at the office building at 8:00, park at the office building, before they leave for the residential community at 18:00, and arrive at the community at 18:30. The daily commuting distance (including forth and back trips) is 40 km/vehicle, and the commuting time is one hour (30 min for each trip). Besides, each HV is \$50000, but the buyers will receive an up to \$15000 subsidy from the Toyota company [32] and another \$4500 subsidy from the California government [33]. Thus, each HV is lowered to about \$35000, which can be afforded by normal families.

To simplify the scenario simulation, some assumptions are proposed:

- (1). The HVs are regarded as H₂ tanks for energy storage and PEMFC for H₂-electricity conversion.
- (2). During transportation procedure, fast power changes can be on the vehicle PEMFCs within seconds [34], and the H₂ consumption of HVs is calculated based on the actual distance (40 km/vehicle and 0.00996 kg/km H₂ consumption rate) and vehicle HVAC

Table 2
Cost information of the local power grid.

Month	Electricity price (\$/kWh)		Demand price (\$/kW)	Annual net surplus electricity reward (\$/kWh)
	Peak period	Off-peak period		
<i>Community</i>				0.03
Jun-Sep	0.36540	0.27044	–	
Jan-May & Oct-Dec	0.29153	0.27415	–	
<i>Office</i>			15.68	–
Jun-Sep	0.19174	0.19174	–	
Jan-May & Oct-Dec	0.15413	0.15413	–	

- energy use (see Section 2.4). The PEMFC power during transportation procedure is determined by the empirical model [35].
- (3). Each vehicle PEMFC has a 4.7 kW idling power [36]. Namely, if the demand shortage power of the office is lower than 4.7 kW, the PEMFCs cannot be activated.
 - (4). For the safety concern, the inner pressure of HV tanks is at least 2 bar higher than the atmospheric pressure. In order to cover the daily transportation demand, the lowest SOC of HV tanks ($SOC_{lower, limit}$) is 0.09. Meanwhile, the upper SOC limit ($SOC_{upper, limit}$) is 0.95.

2.4. Evaluations on vehicle thermal performance and HVAC energy consumption

This study adopts a two-space lumped capacitance thermal network model for evaluating inside temperature of vehicle and HVAC energy consumption [13]. The two-space model (Fig. 3) adopts the physical parameters of Toyota Mirai 2016 [6] and configures two adjacent spaces (cabins), respectively. For each cabin, the heat balance involves the inner heat gain (occupants, PEMFCs, and HVAC system) and the heat transfer from outside to the adjacent cabin. The detailed mathematical models and parameters are presented in [13].

2.5. Inter-city energy migration framework and energy management strategies

As shown in Fig. 4, the proposed inter-city energy migration network includes the office building, HVs, local power grids, H₂ pipelines, and residential community with rooftop PV systems, electrochemical batteries, and an adjacent H₂ station. The main renewable electricity is produced by the rooftop PV systems, which are used to cover residential building demands or stored in the batteries. The power imported from the micro-grid to the H₂ station (G2S interaction) will produce H₂ gas through an electrolyzer and a compressor. The generated H₂ gas is then stored in the high-pressure H₂ tank in the H₂ station. In addition to the renewable generated H₂, another H₂ source of the H₂ station is from the local H₂ pipelines. The renewable energy migration from the residential community to the office building is actualized through HVs' daily transportation. As stated in Section 2.1, the residential community produces more renewable electricity than its demand. The community is equipped with an electric battery for storing electricity when the renewable energy is abundant and covering energy demands when there is demand shortage. With the batteries, the community has relatively low grid loads (usually lower than 20 kW and clarified in Section 3.2.2), which are much lower than the grid loads of the office building (around 50 kW and clarified in Section 3.2.2). Moreover, the maximum power of the vehicle fuel cell is 114 kW, usually higher than the power demand of the residential community. This leads to the ineffectiveness of V2B interaction in the residential community. Thus, the V2B interaction by

discharging the HVs is mainly conducted for covering the demand of the office building. Moreover, two heat recovery systems are adopted to recover waste heat from electrolyzer and PEMFCs to reduce heating loads of the residential building and the office building, respectively. Specifically, the water, which directly cools the electrolyzer during the electrolyzation procedure, is collected and stored in a water tank at the H₂ station, and is then sent to the community for the domestic use. The heat released by vehicle PEMFCs in the V2B interaction is absorbed by PEMFCs' coolant and then injected into the domestic hot water system in the office through non-contact heat transfer. Furthermore, both the community and the office are also connected to their adjacent local power grids to actualize the power balances. Lastly, the potential energy trading among multiple stakeholders is presented by the capital flow (as marked by the grey arrows in Fig. 4), with a contrary direction as the energy flow. The detailed information on the energy trading of the proposed network will be clarified in Section 2.7.

(G2B is the grid-to-building interaction; G2S is the grid-to-H₂-station interaction; S2V is the H₂-station-to-vehicle interaction; V2B is the vehicle-to-building interaction.)

To explore the techno-economic feasibility of the transportation-based energy migration framework through daily commuting with fuel-cell-driven vehicles. Therefore, three cases are proposed:

- (1). The reference case: The office building, residential community, and H₂ station are isolated from each other, corresponding to the current status of regional energy networks in California.
- (2). Case 1: The community is connected to the H₂ station, but no energy migration from the community to the office is deployed. The onsite-renewable-generated H₂ is used to cover transportation energy demand of the HVs with the price same as that of the pipe-delivered H₂ (16.51 \$/kg).
- (3). Case 2: The community is connected to the H₂ station, and the inter-city energy migration from the community to the office is deployed. The onsite-renewable-generated H₂ is used to cover transportation energy demand of the ten HVs and partially to cover the building demand in the V2B interaction process, with the price at 6.5 \$/kg (the pipe-delivered H₂ is still 16.51 \$/kg).

The energy management strategies of the three cases are rule-based, and their control logics are described as follows:

- (1) Reference case (Fig. 5(a)): As the energy prosumer, the community deploys a micro-grid connecting all single houses, rooftop PV systems, electrical batteries, and local power grid, so the renewable electricity by PV panels and the battery storage can be shared by all houses. After the charging or discharging processes from battery storage, the surplus renewable energy or demand shortage of the community will be dynamically balanced by the local power grid. For the office building, as a pure energy consumer, its electricity demand will only be covered by the local power grid. For the whole network, the renewable energy of the community ($P_{REe, com}$) is used to firstly cover the community energy demand ($L_{e, com}$) (Fig. 5(b)):
- (a) If $P_{REe, com}$ is higher than $L_{e, com}$, the surplus renewable ($P_{surp1, com} = P_{REe, com} - L_{e, com}$) is to charge the batteries, before being exported to the local grid. The real dynamic battery charging power ($P_{battery, char}$) is the minimum value between the surplus renewable power ($P_{surp1, com}$) and the upper threshold of battery charging power ($P_{battery, char, max}$).
- (b) If $P_{REe, com}$ is lower than $L_{e, com}$, the community energy demand shortage ($P_{short1, com} = L_{e, com} - P_{REe, com}$) is covered by the electricity discharged from the battery and then by electricity imported from the local grid. The real dynamic battery discharging power ($P_{battery, dischar}$) is the minimum value between the demand shortage power ($P_{short1, com}$) and the upper threshold of battery discharging power ($P_{battery, dischar, max}$).

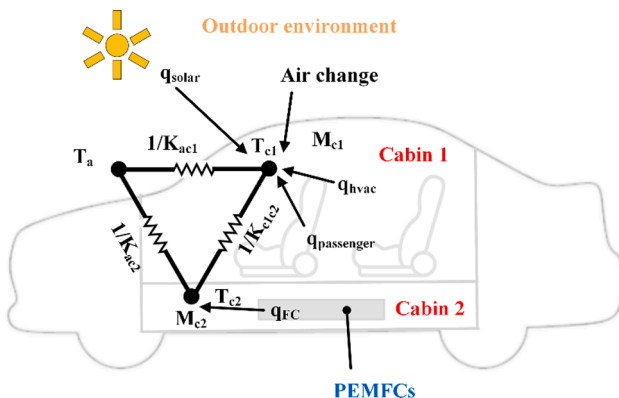


Fig. 3. The two-space cabin thermal model (originally from reference [13]).

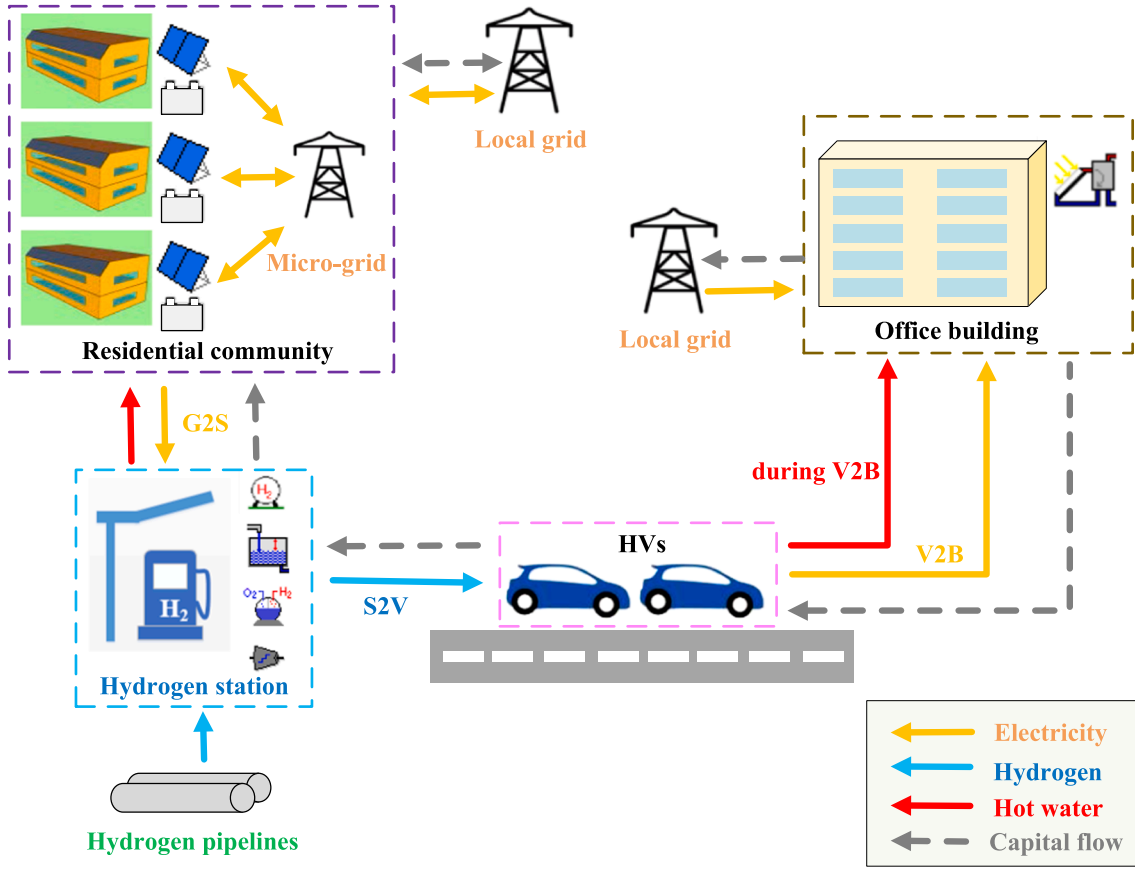


Fig. 4. The configuration of the proposed building-vehicle energy network with transportation-based energy migration framework between a residential community and an office building.

- (c) For the office building, as the energy consumer, the energy shortage ($P_{short1, office}$) is equal to the energy demand ($L_{e, office}$), and is only covered by the local grid.
- (2) Case 1 (Fig. 6(a)): compared to the reference case, Case 1 adds a connection between the micro-grid and the adjacent H₂ station. The renewable energy can be sent to the H₂ station for H₂ production to cover daily transportation energy demands. This can help to mitigate the renewable congestion pressure on the local grid, since a large amount of renewable electricity is converted to H₂ gas, instead of being exported into the local grid. However, no inter-city energy migration strategy is deployed, and no renewable energy is transferred from the community to the office building through the HVs.
- (a) If $P_{REe, com}$ is higher than $L_{e, com}$, the surplus renewable ($P_{surp1, com}$) is to charge the battery, then to H₂ system, and finally exported to the local grid. The real dynamic battery charging power ($P_{battery, char}$) is the minimum value between the surplus renewable power ($P_{surp1, com}$) and the upper threshold of battery charging power ($P_{battery, char, max}$). The magnitude of the second-order surplus renewable ($P_{surp2, com} = P_{surp1, com} - P_{battery, char}$) determines whether it will be exported to the H₂ system or local grid. To be specific, if $P_{surp2, com}$ is lower than the sum of the electrolyzer idling power ($P_{ely, idling}$) and the compressor power (P_{comp}), it is exported to the local grid, as it cannot activate the H₂ system for H₂ production. Moreover, if $P_{surp2, com}$ exceeds the sum of P_{ely} and P_{comp} , the third-order excessive renewable ($P_{surp3, com} = P_{surp2, com} - P_{ely, idling} - P_{comp}$) will be exported to the local power grid.
- (b) If $P_{REe, com}$ is lower than $L_{e, com}$, the energy flow for covering $P_{short1, com}$ is the same as that in the reference case.
- (c) For the office building, as an energy consumer, the energy demand is still only covered by the local power grid.
- (4) Case 2 (Fig. 7(a)): compared to Case 1, Case 2 additionally deploys the proposed inter-city energy migration framework through HVs to cover the energy demand of the office building. The maximum output power of a vehicle PEMFC for covering energy shortage is dependent on the designed maximum power (114 W) and the magnitude of fuel cell degradation. For the whole network, $P_{REe, com}$ is used to firstly cover $L_{e, com}$ (Fig. 7(b)):
- (a) If $P_{REe, com}$ is higher than $L_{e, com}$, the excessive renewable ($P_{surp1, com}$) follows the same power flow principle as that of Case 1.
- (b) If $P_{REe, com}$ is lower than $L_{e, com}$, the power flow for covering $P_{short1, com}$ also follows the same flow principle as that of Case 1.
- (c) For the office building, when there are HVs parking nearby, $P_{short1, office}$ can be covered by the V2B interaction, when multiple constraints are satisfied, i.e., $P_{short1, office}$ higher than the vehicle PEMFCs' idling power ($P_{FC, idling}$), the accumulated onsite-renewable-generated H₂ available ($H_{2RE, store} > 0$), and the SOC_{HV} higher than $SOC_{lower, limit}$ simultaneously. Otherwise, $P_{short1, office}$ is covered by the imported electricity from the local grid.

2.6. Key parameters of the district energy system

In this study, Python programming language (Python 3.8) is used to build the dynamic models of HV heat transfer and fuel cell degradation, and TRNSYS Types [37] are used to develop the energy components of the entire energy sharing network including H₂ tanks, PEMFCs, PV panels, and so on. The simulation time step is 0.25 h. The key parameters of each energy component are shown in Table 3.

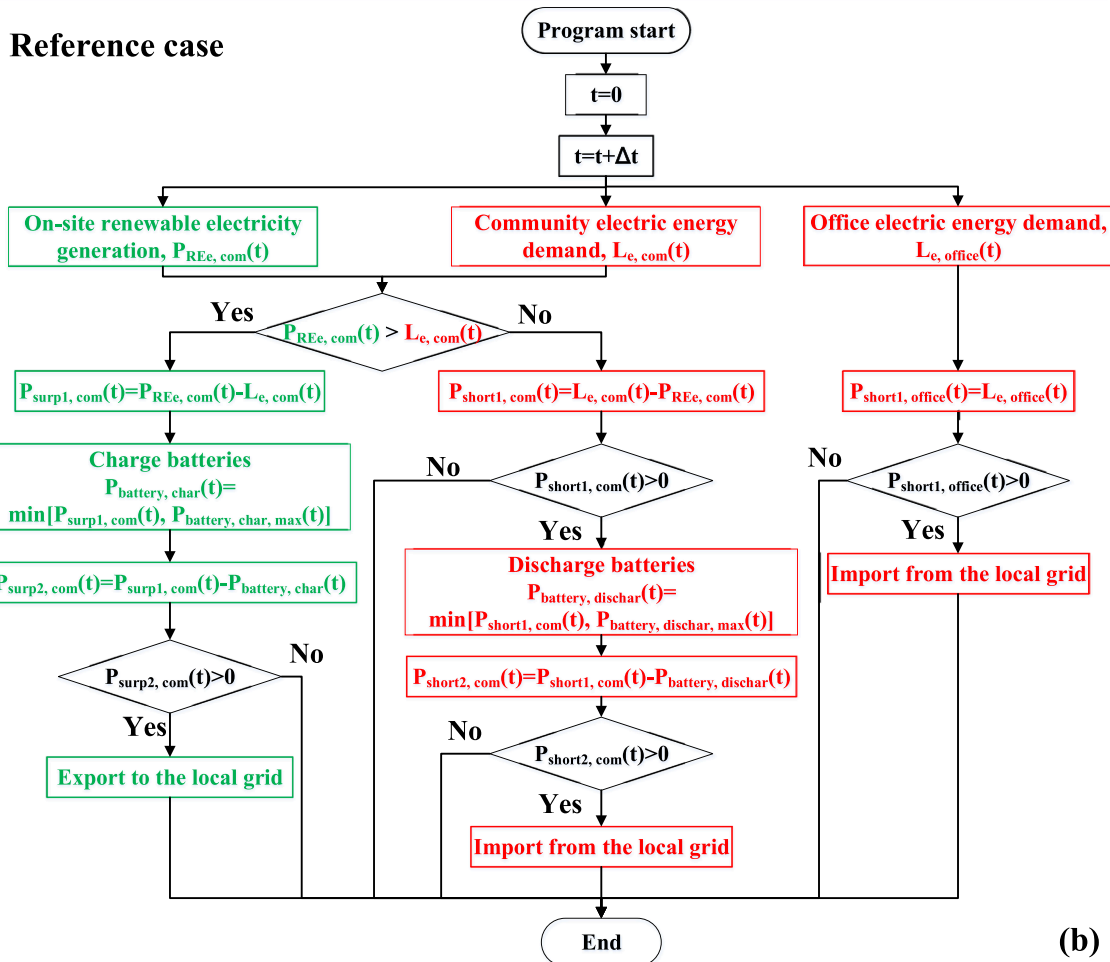
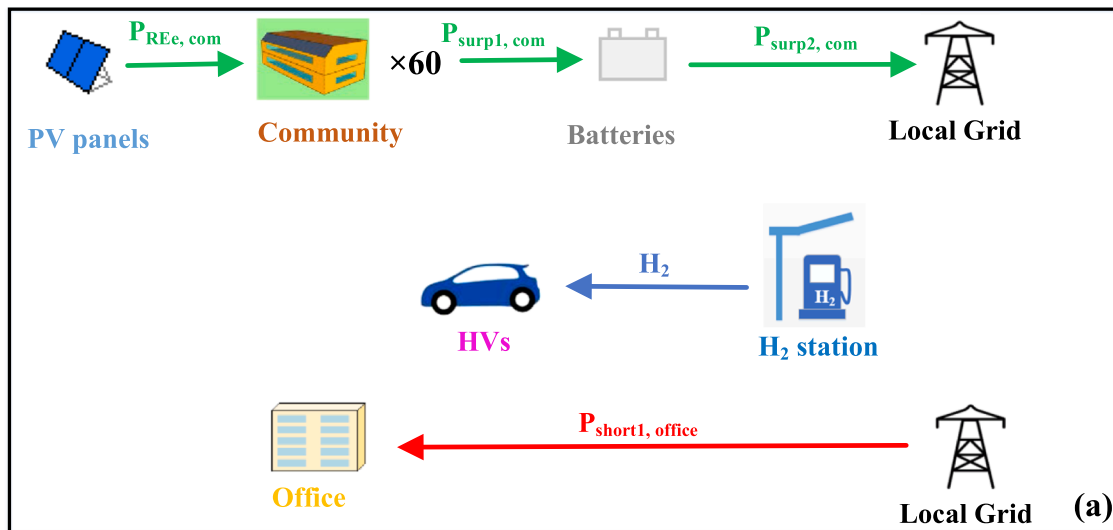


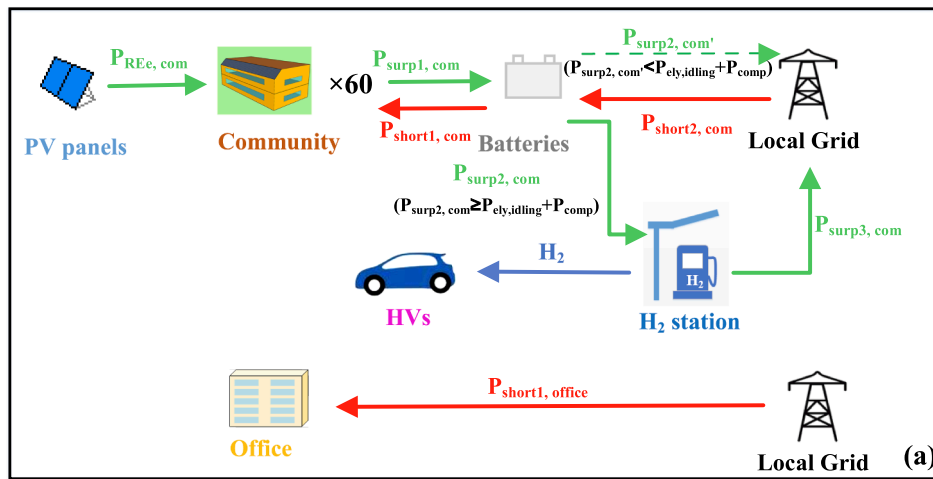
Fig. 5. (a) The energy flow and (b) the rule-based control logic of the proposed building-vehicle network in the reference case.

2.7. Multi-stakeholder energy trading in the inter-city energy migration network

As shown in Fig. 4, the proposed inter-city energy migration network involves five stakeholders: the residential house owners, office building owner, HV owners, H₂ station, and local power company. The arrows show the capital flow (payment) among stakeholders. Besides the energy trading between the community/office building and the local grid, the energy trading of the network includes:

- (1) The energy trading between the community and the H₂ station, for the renewable electricity transmitted from the community to the H₂ station for H₂ production;
- (2) The energy trading between the H₂ station and HV owners, when HVs are charged at the H₂ station;
- (3) The energy trading between the office building and the HV owners, to meet the demand of the office.

A sustainable and feasible multi-stakeholder energy network should



Case 1

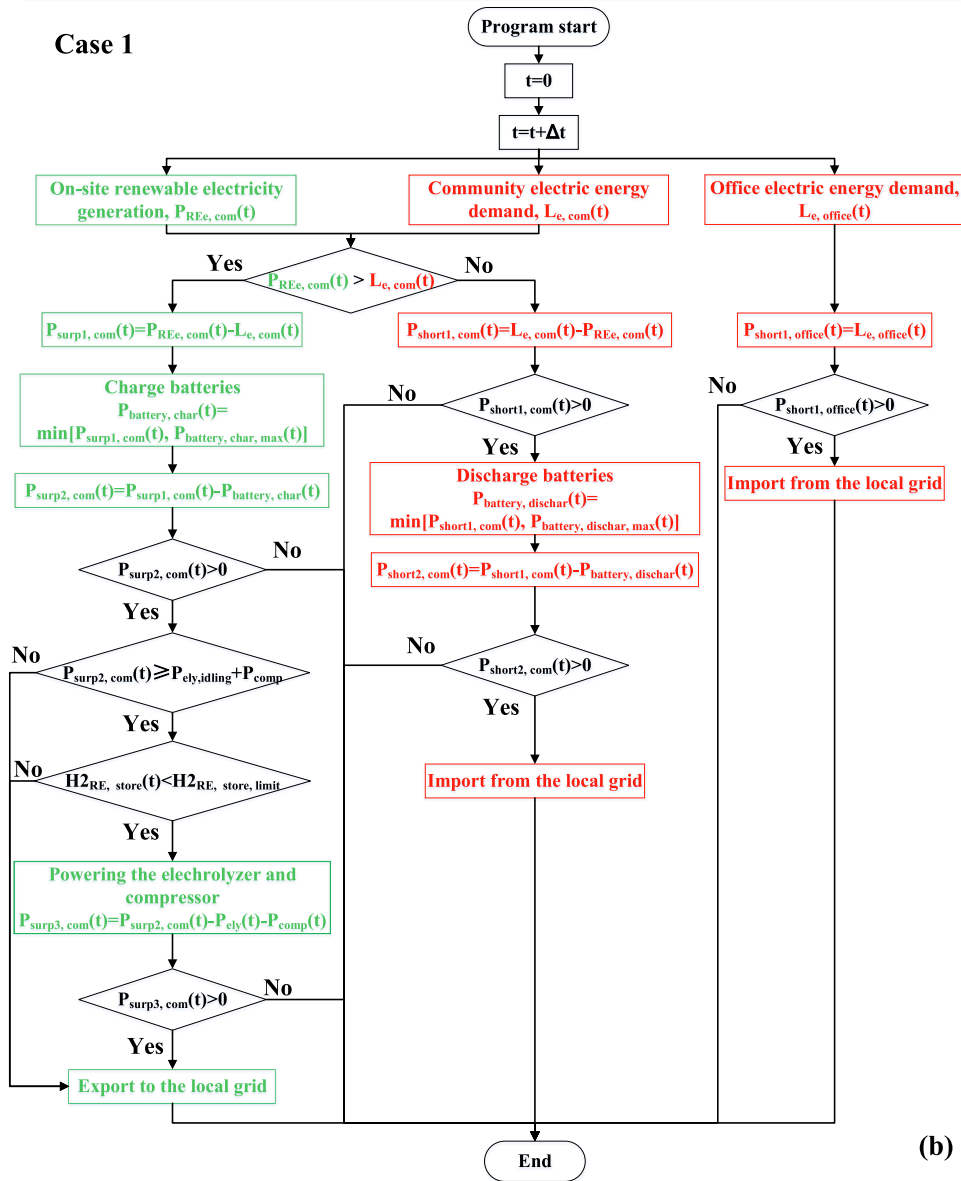
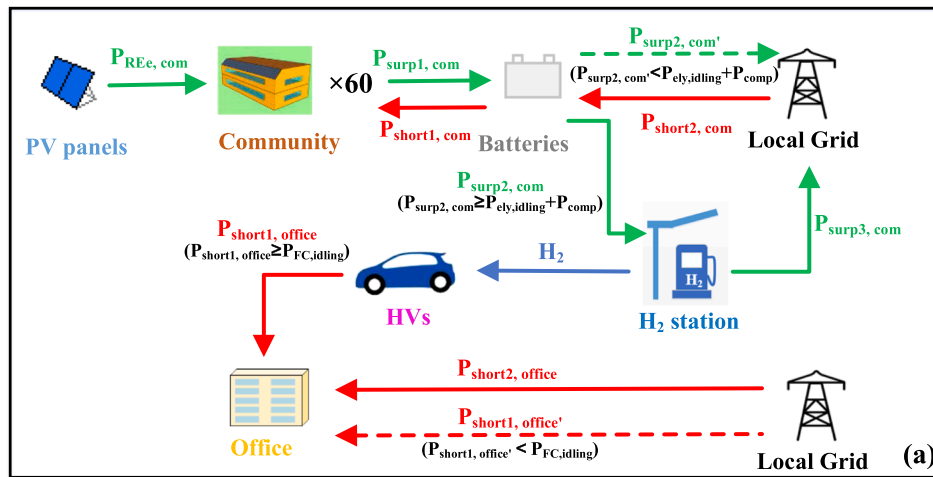


Fig. 6. (a) The energy flow and (b) the rule-based control logic of the proposed building-vehicle network in Case 1.



Case 2

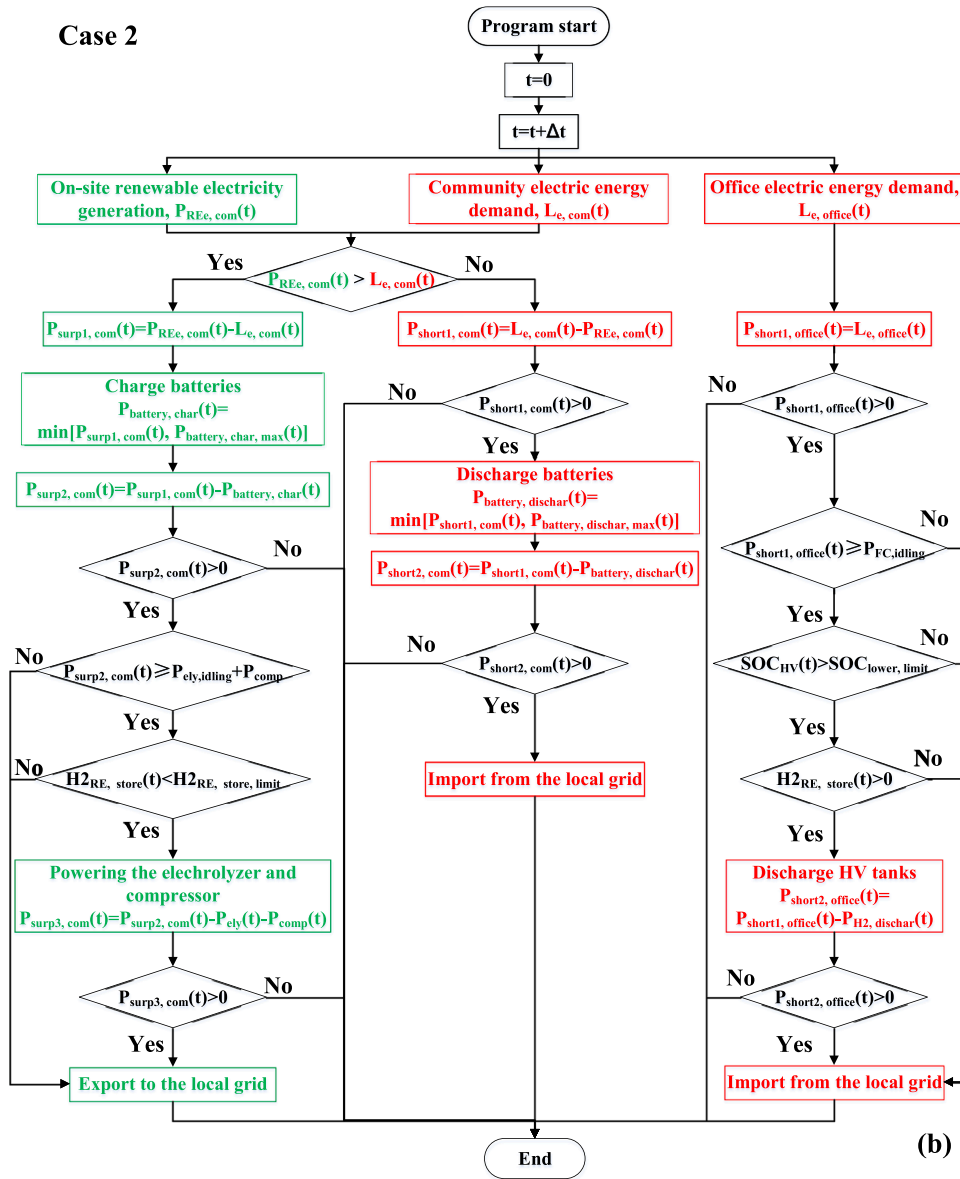


Fig. 7. (a) The energy flow and (b) the rule-based control logic in Case 2.

Table 3
Key parameters in TRNSYS.

Components	Parameters	Value
PV panels	Type	567
	Length and width (m)	20 and 2
	Temperature coefficient ($^{\circ}\text{C}$)	-0.003
	Reference PV efficiency	0.22 [38]
	Channel height (m)	0.1
Electrolyzer	Type	160a
	Electrode area (m^2)	0.5
	Number of cells per stack and number of stacks	20 and 2
	Operating temperature ($^{\circ}\text{C}$)	80
Compressor	Type	167
	Desired pressure (bar)	700
	Number of parallel compressors and compressor stages	1 and 3
HV hydrogen tank (ten HVs)	Type	164b
	Maximum pressure (bar)	700
	Tank volume (m^3)	1.22
PEMFC	Type	170a
	Number of cells per stack and number of stacks	60 and 6
	Electrode area (cm^2)	1000
H ₂ station	Type	Self-developed
	Maximum stored onsite-renewable-produced H ₂ (kg)	500
Water heater	Type	138
	Set-point temperature of domestic hot water ($^{\circ}\text{C}$)	49
	Set-point temperature for space heating ($^{\circ}\text{C}$)	45
	Type	5
Heat exchanger (for two-stage cooling)	Load side inlet temperature ($^{\circ}\text{C}$)	20
	Overall heat transfer coefficient ($\text{W}/\text{m}^2\cdot\text{K}$)	2000
	Type	534
Water tank (office heating and cooling)	Volume (m^3) and height (m)	20 and 2
	Heat loss coefficient ($\text{W}/\text{m}^2\cdot\text{K}$)	0.5
	Type	655
Chiller	Rated capacity (kW)	300
	Rated COP	4
	Set Point Temperature ($^{\circ}\text{C}$)	7
	Type	71
Solar thermal panel	Collector area (m^2)	200
	Collector slope ($^{\circ}$)	45
	Collector azimuth ($^{\circ}$)	0

globally ensure that every stakeholder receives economic benefits by participating in the network, rather than only locally focusing on the total operating cost. For example, the HV owners are willing to participate in the transportation-based energy migration framework, only when the payment of vehicle PEMFC powering the office building exceeds the sum cost of the additional H₂ consumption and the fuel cell degradation by V2B interactions.

From the perspectives of sustainability and practical feasibility, the energy trading (1) between the community and the H₂ station is feasible only when the community receives more rewards to sell renewable energy to the H₂ station than other strategies, and simultaneously the H₂ station has a lower cost of renewable-driven H₂ than the pipe-delivered H₂. This study assumes that the renewable-driven H₂ and the pipe-delivered H₂ have the same H₂ production and storage costs, but the onsite-renewable-generated H₂ has no transportation cost compared to that of the pipe-delivered H₂. Therefore, the energy trading (1) is acceptable for the H₂ station, if the payment to the community for the renewable-driven H₂ production is less than the H₂ pipe-delivery cost. It is assumed that the pipeline-delivered H₂ will be provided by a H₂ production plant with a daily H₂ production capacity of 11000 kg, located in Lancaster, south of California [39], which is about 600 km

from the San Francisco Bay Area. According to the method of the U.S. Department of Energy, the H₂ pipe-delivery cost from Lancaster to the Bay Area is 2.39–5.96 $\$/\text{kg}$ [40], and it is set at 4.5 $\$/\text{kg}$ in this study.

The energy trading (2) between the H₂ station and HV owners is feasible, only when the HV owners have lower costs when participating in the trading scheme than that of the scenario without participation.

The energy trading (3) between the office building and the HV owners is feasible only when the office building has a lower electricity cost when participating in the transportation-based energy migration framework than the scenario without participation.

To enable the economic sustainability of the transportation-based energy migration framework, all above-mentioned energy trading schemes and constraints need to be satisfied, simultaneously. Since the energy trading does not change the energy flow of the whole energy network, once the energy management strategy has been decided, the specific analysis on energy trading is arranged in Section 3.4, after the analysis on the energy flexibility and grid interaction (Sections 3.2 and 3.3). In the energy trading analysis, the energy trading price thresholds are explored for the economic feasibility of the proposed energy network.

2.8. Performance metrics

2.8.1. Energy self-sufficiency and renewable energy self-use

Energy independence of both the residential community and the office building is evaluated by the energy self-sufficiency ratio (SSR), which is the fraction of annual energy demand covered by onsite or stored renewable energy ($0 \leq \text{SSR} \leq 1$) [41]. If SSR is 1, 100 % of the energy demand of a building or community is covered by renewables. If SSR is 0, the energy demands of buildings are completely covered by energy imported from power grid.

$$\text{SSR} = \frac{\int_0^{t_{\text{end}}} \text{Min}[P_{\text{REe}}(t) + P_{\text{V2B}}(t) + P_{\text{HW, stored}}(t), L_e(t)] dt}{\int_0^{t_{\text{end}}} L_e(t) dt} = 1 - \frac{\int_0^{t_{\text{end}}} P_{\text{imp}}(t) dt}{\int_0^{t_{\text{end}}} L_e(t) dt} \quad (9)$$

where $P_{\text{REe}}(t)$ is the renewable energy power at the t -th time step (kJ/h), and it is zero for the office building; $P_{\text{V2B}}(t)$ is the V2B interaction power at the t -th time step (kJ/h), and it is zero for the community; $P_{\text{HW, stored}}(t)$ is the recovered heat at the t -th time step (kJ/h); $L_e(t)$ is the energy demand power (the residential community or the office building) at the t -th time step (kJ/h); P_{imp} is the grid-import power at the t -th time step (kJ/h); t is the time step (h); t_{end} is the ending time of simulation (the 8760th hour herein).

The renewable self-use ratio (SUR), which is the ratio of renewables directly to cover demands and absorbed by energy storage to the total renewable production ($0 \leq \text{SUR} \leq 1$), is adopted to evaluate the renewable self-use ratio of the community. If SUR is 1, it means that all the renewable energy is used directly used or stored rather than being exported to the grid.

$$\text{SUR} = \frac{\int_0^{t_{\text{end}}} \text{Min}[L_e(t) + P_{\text{to battery}}(t) + P_{\text{to H2}}(t), P_{\text{REe}}(t)] dt}{\int_0^{t_{\text{end}}} P_{\text{REe}}(t) dt} = 1 - \frac{\int_0^{t_{\text{end}}} P_{\text{exp}}(t) dt}{\int_0^{t_{\text{end}}} P_{\text{REe}}(t) dt} \quad (10)$$

where $P_{\text{to battery}}(t)$ is the renewable energy power for charging electrochemical batteries (kJ/h); $P_{\text{to H2}}(t)$ is the renewable energy power absorbed by the electrolyzer and compressor (kJ/h); P_{exp} is the grid-export power at the t -th time step (kJ/h).

2.8.2. Grid interaction

The function of the local micro-grid is to dynamically balance the power supply and demand of residential community and the office building, with dynamic grid-import power (P_{imp}) and the grid-export power (P_{exp}). The low grid-import power (P_{imp}) and the grid-export power (P_{exp}) indicate the low burdens and low fluctuation on the

micro-grid.

2.8.3. Energy operating cost

The energy operating cost of the proposed inter-city building network involves the costs of grid-imported electricity, H₂ charged to the HVs, and fuel cell degradation, and the rewards by V2B interaction and renewable H₂ production.

Based on the information in Table 2, the annual grid-import cost (IC , \$/a) and the annual grid-exported electricity compensation (EC , \$/a) are calculated as follows:

$$IC_{peak,mon,i} = E_{imp,peak,mon,i} \times R_{peak,mon,i} \quad (11)$$

$$IC_{off-peak,mon,i} = E_{imp,off-peak,mon,i} \times R_{off-peak,mon,i} \quad (12)$$

$$IC = \sum_{i=1}^{12} (IC_{peak,mon,i} + IC_{off-peak,mon,i}) \quad (13)$$

$$EC_{peak,mon,i} = E_{exp,peak,mon,i} \times R_{peak,mon,i} \quad (14)$$

$$EC_{off-peak,mon,i} = E_{exp,off-peak,mon,i} \times R_{off-peak,mon,i} \quad (15)$$

$$EC = \sum_{i=1}^{12} (EC_{peak,mon,i} + EC_{off-peak,mon,i}) \quad (16)$$

For each year, the electricity cost ($C_{e,1}$, \$/a) is decided by the grid-imported cost and grid-exported compensation:

$$C_{e,1} = \begin{cases} IC - EC & \text{if } IC > EC \\ 0 & \text{if } IC \leq EC \end{cases} \quad (17)$$

For the community, the annual net grid-electricity consumption ($E_{net,annual}$) is calculated below:

$$E_{net,annual} = \int_0^{t_{end}} P_{imp}(t) dt - \int_0^{t_{end}} P_{exp}(t) dt \quad (18)$$

Additional reward for grid feed-in tariff ($C_{e,2}$, \$/a) is calculated below:

$$C_{e,2} = \begin{cases} (-E_{net,annual}) \times 0.03 & \text{if } E_{net,annual} < 0 \\ 0 & \text{if } E_{net,annual} \geq 0 \end{cases} \quad (19)$$

The additional reward by the annual net renewable electricity exportation to the H₂ station for H₂ production ($C_{e,3}$, \$/a) is calculated below:

$$C_{e,3} = \int_0^{t_{end}} P_{toH2}(t) dt \times R_{H2production} \quad (20)$$

where P_{toH2} is renewable power exported to the H₂ system (kW); $R_{H2production}$ is the reward rate of exporting renewable electricity to the H₂ station for H₂ production (\$/kWh).

The total annual energy operating cost of the residential community ($C_{e,comb}$, \$/a) is calculated as follows:

$$C_e = C_{e,1} - C_{e,2} - C_{e,3} \quad (21)$$

For the office building, it needs to include the power demand cost ($C_{e,4}$, \$/a) according to its maximum monthly grid-import power:

$$PC_{mon,i} = P_{imp,max,mon,i} \times R_{peakpower} \quad (22)$$

$$C_{e,4} = \sum_{i=1}^{12} PC_{mon,i} \quad (23)$$

where $PC_{mon,i}$ is the cost of the grid power demand of the i -th month (\$); $P_{imp,max,mon,i}$ is the maximum grid-import power of the i -th month (kW); $R_{peakpower}$ is the power demand price.

Additionally, according to Section 2.8, the office building also has the cost for using the electricity provided by V2B interactions ($C_{e,5}$, \$/a):

$$C_{e,5} = \int_0^{t_{end}} P_{V2B,kW}(t) dt \times R_{V2B} \quad (24)$$

where $P_{V2B,kW}$ is V2B interaction power in kW; R_{V2B} is the reward rate of V2B interactions for covering building energy demands (\$/kWh).

The total annual grid cost of the office building ($C_{e,office}$, \$/a) is calculated as follows:

$$C_{e,office} = C_{e,1} + C_{e,4} + C_{e,5} \quad (25)$$

In the reference case and Case 1 without V2B interaction, the annual cost of H₂ (C_{H2} , \$/a) is calculated below:

$$C_{H2} = 16.51 \times \int_0^{t_{end}} M_{HVtran,H2}(t) dt \quad (26)$$

where $M_{HVtran,H2}(t)$ is the H₂ consumption for transportation (kg/h).

In Case 2 with V2B interaction, when the annual onsite-renewable-produced H₂ amount is higher than that used for daily transportation and V2B interactions, the annual cost of H₂ (C_{H2} , \$/a) is calculated below:

$$C_{H2} = 4 \times \int_0^{t_{end}} [M_{HVtran,H2}(t) + M_{V2B,H2}(t)] dt \quad (27)$$

where $M_{V2B,H2}(t)$ is H₂ consumption for V2B interaction (kg/h); 4 is the price of the onsite-renewable-produced H₂.

In Case 2 with V2B interaction, when the annual onsite-renewable-produced H₂ amount is lower than that used for daily transportation and V2B interactions, C_{H2} , \$/a is calculated below:

$$C_{H2} = 4 \times \int_0^{t_{end}} M_{H2,onsite}(t) dt + 16.51 \times \int_0^{t_{end}} [M_{HVtran,H2}(t) + M_{V2B,H2}(t) - M_{H2,onsite}(t)] dt \quad (28)$$

where $M_{H2,onsite}(t)$ is the onsite-renewable-produced H₂ at the t -th time step (kg/h). 16.51 is the price of the pipe-delivered H₂.

The total degradation by V2B interactions ($D_{FC,V2B,total}$) is assumed to be averagely shared by all the HVs participating in V2B interactions [13]. Thus, for each HV, the fuel cell degradation (D_{FC}) is:

$$D_{FC} = D_{FC,HVtran} + D_{FC,V2B,total}/n_{HV} \quad (29)$$

Where $D_{FC,HVtran}$ is fuel cell degradation by daily transportation. n_{HV} is the quantity of HVs participating in V2B interactions.

The fuel cell degradation cost is calculated with the assumption that (1) each vehicle's PEMFC is \$11000 [42] and (2) each PEMFC must be replaced when its degradation reaches 20%. Thus, every 1% decrease in a vehicle PEMFC will increase the degradation cost by \$550. The annual cost of fuel cell degradation (C_{FC} , \$/a) of HVs is calculated as follows:

$$C_{FC} = D_{FC} \times n_{HV} \times 550 \quad (30)$$

The total annual energy operating cost of HVs (C_{HV} , \$/a) is calculated below:

$$C_{HV} = C_{H2} + C_{FC} - C_{e,5} \quad (31)$$

3. Results

3.1. Annual energy demands of the inter-city energy migration network

The annual energy demand of the residential community is 526145.2 kWh (21.9 kWh/m²·a), and the renewable electricity generation is 736288.1 kWh (30.7 kWh/m²·a). Namely, for each household, the average energy demand and renewable generation are 8769.1 and 12271.5 kWh, respectively. The annual H₂ consumption for transportation is 105.0 kg H₂ per vehicle, corresponding to a total travel

distance of 10040 km per vehicle. The annual energy demand of the office building is 189468.0 kWh (37.9 kWh/m²·a).

3.2. Impact of transportation-based energy migration framework on techno-economic performance

In Section 3.2, impact of transportation-based energy migration framework on grid independence, renewable self-use ratio, grid stability, and operating cost was analyzed. The objective is to provide qualitative results on the formulated transportation-based energy migration framework. Note that, due to the complexity and multiple stakeholders, the energy trading between the community and H₂ station, and between HV owners and the office building is not considered. Namely, the energy costs do not include those caused by exporting renewable electricity to the H₂ station and V2B interactions.

3.2.1. Improvements in energy independence and renewable self-use ratio

Fig. 8 illustrates the energy self-sufficiency ratios (SSR) and renewable self-use ratios (SUR) of the inter-city energy migration network under three cases. It can be noticed that the transportation-based energy migration framework enhances the energy independence of the office building and the renewable energy use efficiency of the residential community. To be specific, due to the isolation among the community, office building and H₂ station in the reference case, the SSR values of the community and office building are 0.812 and 0, meaning that 81.2 % of the energy demand of the community is covered without importing electricity from the grid (1.52 × 10⁹ kJ electricity from the rooftop PV panels and electrochemical batteries vs. 1.89 × 10⁹ kJ electrical annual energy demand) and the electrical demand of the office is fully covered by the electricity from the local power grid. Meanwhile, the SUR value of the community rooftop PV systems is 0.727, meaning that 72.7 % of the renewable electricity by the rooftop panels is directly used by the community houses or stored in the electrochemical batteries (1.93 × 10⁹ kJ directly used or stored vs. 2.65 × 10⁹ kJ total renewable generation). In Case 1 where the community is connected to the nearby H₂ station through the micro-grid, but still isolated from the office building, the SSR value of the community slightly decreases to 0.800. This is because that, a considerable amount of renewable electricity absorbed by the H₂ system in the H₂ station (2.98 × 10⁸ kJ) reduces the amount of renewable electricity stored in the batteries to cover the community's energy demand (battery-stored renewable energy: 1.31 × 10⁹ kJ in Case 1 and 1.34 × 10⁹ kJ in the reference case). Meanwhile, due to the renewable electricity absorbed by the H₂ system (2.98 × 10⁸ kJ), the SUR value increases from 0.727 to 0.828. However, as the pure energy consumer, the office's SSR value is still zero. In Case 2 under the transportation-based energy migration framework, the community SSR slightly

decreases to 0.779 (1.47 × 10⁹ kJ electricity from the rooftop PV panels and electrochemical batteries vs. 1.89 × 10⁹ kJ annual energy demand) due to an increased amount of renewable energy penetrated to the H₂ system (7.67 × 10⁸ kJ) and a decreased amount of renewable charged to the batteries (1.26 × 10⁹ kJ). Meanwhile, due to the transportation-based energy migration framework, the SSR value of the office building is 0.232 in Case 2 (1.58 × 10⁸ kJ electricity provided by V2B interactions vs. 6.82 × 10⁸ kJ total electrical energy demand), and the community SUR value is 0.986 (2.61 × 10⁹ kJ renewable directly used or stored vs. 2.65 × 10⁹ kJ total renewable generation), meaning that only 1.4 % of the renewable energy is exported to the power grid. The results above indicate that the transportation-based energy migration framework significantly enhances grid independence of the office building and renewable self-use ratio of the residential community.

3.2.2. Grid stability enhancement

Fig. 9 illustrates the dynamic grid power responses under the three cases, presented by the mean hourly power. The positive and the negative value refer to the grid-import and grid-export power, respectively. The results in Fig. 9 indicate that the transportation-based energy migration framework contributes to releasing the renewable congestion in the local power grid by the 'energy prosumer'- community, and reduces the grid import pressure by the 'energy consumer'- office. In the

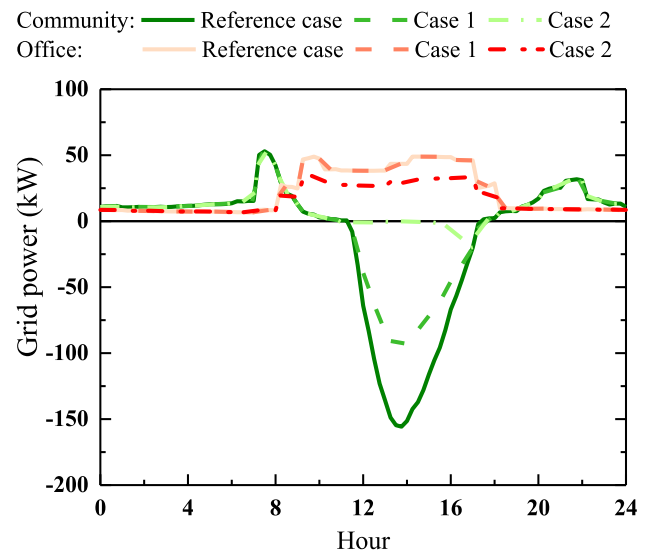


Fig. 9. Grid powers of the residential community and the office building.

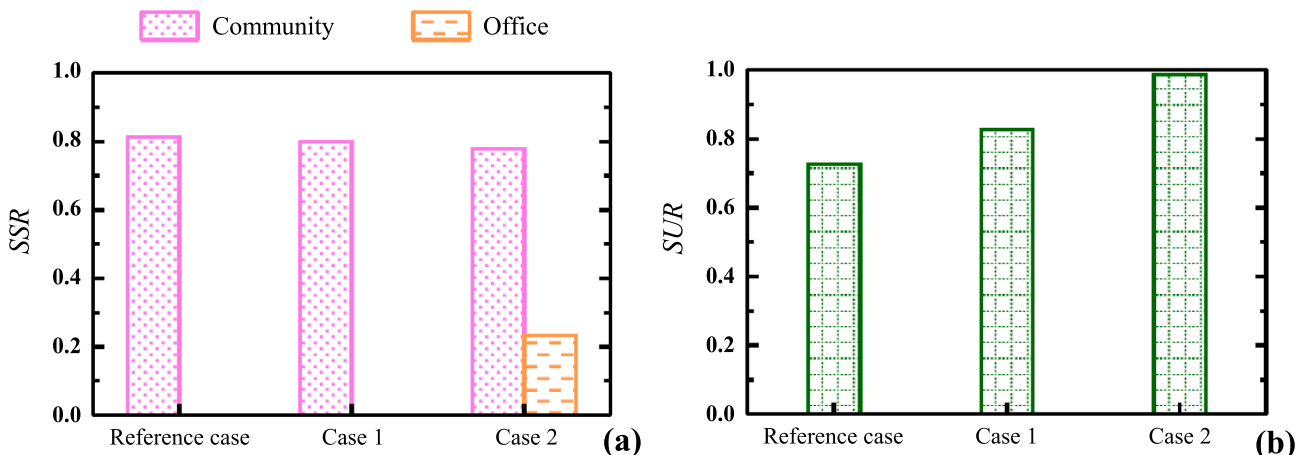


Fig. 8. Comparative analysis on three cases (a) energy self-sufficiency ratio (SSR) and (b) renewable self-use ratio (SUR).

reference case, during the daytime, the maximum grid-export power of the community is 155.7 kW, and the maximum grid-import power of the office is 49.0 kW. In Case 1, where the community and H₂ station are integrated, the renewable congestion of the community during the daytime is significantly reduced, with the maximum grid-export power decreased to 94.0 kW. Nonetheless, since no interaction is deployed between the community and office building, the grid-import power of the office building does not change. In Case 2, where V2B interactions are deployed, the grid-export power of the community decreases to 20.4 kW, indicating that the grid renewable congestion is reduced by 86.9 % compared to the reference case. Meanwhile, the maximum grid-import power of the office building is 34.6 kW, indicating that the grid demand burden is reduced by 29.4 % compared to the reference case. The reason for the enhanced grid stability in Case 2 is due to the H₂ energy storage and transportation-based energy migration framework. To be specific, in Case 2, 7.67×10^8 kJ renewable energy is absorbed by the H₂ system for H₂ gas production, which is about 29 % of the total renewable energy and finally produces 3652.6 kg H₂. Meanwhile, 73 % of the onsite-renewable-produced H₂ is consumed by V2B interactions which provide 46253.4 kWh electricity to the office building (covering 23.2 % of the total energy demand of the office, see Section 3.2.1). In Case 1, the integration of the community and H₂ station has relatively weaker effects on the renewable congestion, compared to that of Case 2. This is because of the much less renewable energy absorbed by the H₂ system in Case 1 (2.98×10^8 kJ renewable energy, about 39 % of that in Case 2) for supporting daily transportation of the ten HVs (producing only 1429.1 kg H₂).

3.2.3. Operating cost of the inter-city energy migration framework

Fig. 10 shows the annual energy operating costs under the three cases, without considering vehicle-building and building-station energy trading. Namely, the results shown in Fig. 10 do not include the costs or benefits caused by building to H₂ station (B2S) and V2B interactions. The main finding is that the transportation-based energy migration framework reduces the energy operating costs of the office building and HVs, but increases the grid-import cost of the residential community. For the residential community, in the reference case, the grid-import cost of the community can be completely compensated, and the community receives an extra payment for its surplus grid-exported renewable electricity (\$3076.2). The reason is due to the high compensation price of grid feed-in tariff [30] and overflowing renewable electricity to the local grid (see Section 3.2.1). In Case 1, the community receives less payment by exporting surplus renewable energy to the local power grid (\$856.1) than the reference case, due to the exportation of renewable electricity to the H₂ station. In Case 2, the grid-import cost of the residential community increases to \$24261.6 because a considerable

amount of renewable electricity is consumed for H₂ production, and less renewable energy is stored by the batteries for covering energy demands or exported to the local power grid. For the office building, in the reference case and Case 1, the demand shortage is covered by the local power grid and the grid-import cost is \$52791.3. In Case 2 where the transportation-based energy migration framework is deployed, the corresponding grid-import cost decreases to \$44154.7, 16.4 % lower than that in the reference case or Case 1.

In terms of the HVs, in the reference case and Case 1, the H₂ is only for supporting daily transportation and the H₂ cost of the ten HVs is \$17336.8. Meanwhile, the average fuel cell degradation is 1.79 % per vehicle and the total degradation cost of the ten HVs is \$9835.7. In Case 2, due to the V2B interactions for covering the energy demand of the office building, more H₂ is produced and consumed (see Section 3.2.1). But due to the cheap-renewable-H₂ policy in Case 2 for encouraging HV owners to participate in V2B interactions, the H₂ cost is \$15767.0, which is \$1569.8 lower than those in the reference case and Case 1. Meanwhile, due to the V2B interaction, the average fuel cell degradation increases to 1.99 % per vehicle, and the additional fuel cell degradation cost by V2B interactions is \$1104.7, which is lower than the H₂ cost reduction from the cheap-renewable-H₂ policy (\$1569.8). Therefore, even with the fuel cell degradation cost, the total energy operating cost of HVs can be lower (1.7 %) than that of the reference case if the HV owners participate in the proposed inter-city energy migration framework, which enhances the economic feasibility and improves the participation willingness of HV owners in the inter-city energy migration network.

3.3. Effects of different grid-regulation strategies on techno-economic performances of vehicle-to-building interaction

An existing problem in Section 3.2 is the significant increase of grid-import cost of the community. Based on the discussion results in Section 3.2, an existing problem can be noticed in Case 2 under the transportation-based energy migration framework, i.e., due to the sharing of large amounts of renewable electricity from the residential community to the H₂ station and office, the grid-export cost of the residential community significantly decreases, leading to the significant decrease in compensating the grid-import cost of the residential community. To improve the economic benefit of the residential community, novel grid-regulation strategies have been proposed, to reduce the peak power of the office building and achieve the cost-saving from peak power reduction (see Table 2).

The grid-regulation strategies are proposed from two aspects [43] and are deployed in Case 2:

- (1) Peak-shaving strategy: besides the energy control strategy, as shown in Fig. 7, an additional constraint on the power threshold of V2B interactions is added. Namely, V2B interactions will be activated only when the energy demand shortage is higher than the minimum power threshold ($P_{V2B, \text{thres, min}}$). By applying the peak-shaving strategy, instead of covering the demand shortage at all ranges, the V2B interactions will only cover high loads (above the $P_{V2B, \text{thres, min}}$) of the demand shortage, aiming to shave the peak power.
- (2) Load-shaping strategy: besides the minimum power threshold ($P_{V2B, \text{thres, min}}$) of V2B interactions added in the peak-shaving strategy, a maximum power magnitude of vehicle PEMFCs for V2B interactions ($P_{V2B, \text{mag, max}}$) is added, to limit the maximum power magnitude in the V2B interaction and prolong the time-duration of the V2B interaction. By deploying the load-shaping strategy, the V2B interactions only partly cover the high demand shortage at each time step, but prolong the time-duration of the V2B interaction. The benefit of the strategy is to reduce the time-duration of peak value of grid-import power through the V2B interaction.

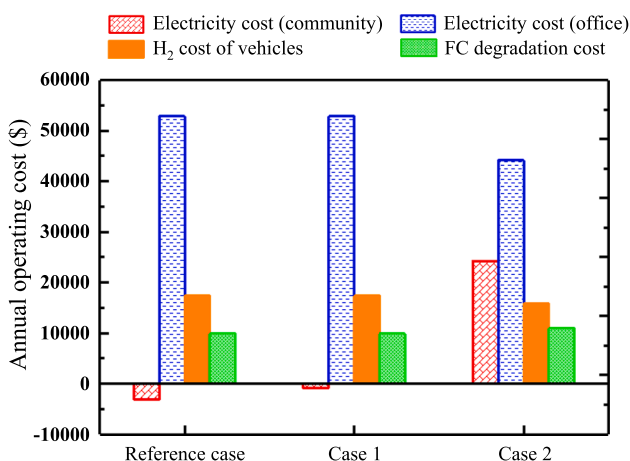


Fig. 10. Energy operating costs of the community, office, and HVs under the three cases.

3.3.1. Peak-shaving strategy

To quantify the effects of the peak-shaving strategy on grid power and system operating cost, the $P_{V2B, \text{thres, min}}$ value is set from 20 to 70 kW, with an interval of 10 kW. Fig. 11(a) illustrates the evolution of the mean hourly grid power, with different $P_{V2B, \text{thres, min}}$. The main finding is that the elevated power threshold of V2B interactions increases the local power grid burden, but decreases the energy operating costs of the community and HVs. When the $P_{V2B, \text{thres, min}}$ value increases from 20 to 70 kW, the grid-export power of the community increases from 20.4 kW to 90.6 kW, since less renewable-generated H_2 is consumed for V2B interactions. For example, when the $P_{V2B, \text{thres, min}}$ value is set at 20 kW, 2550.8 kg H_2 is consumed by V2B interactions for covering office energy shortage, and 1.31×10^4 kWh renewable electricity is exported to the local grid. When the $P_{V2B, \text{thres, min}}$ value is set at 70 kW, 179.4 kg H_2 is consumed by V2B interactions, and 1.21×10^5 kWh renewable electricity of the community is exported to the local grid. Simultaneously, when the $P_{V2B, \text{thres, min}}$ value increases from 20 to 70 kW, the grid-import power of the office building increases from 36.9 kW to 47.7

kW due to the reduced amount of H_2 for V2B interactions. Moreover, as shown in Fig. 11(b), with the increase in $P_{V2B, \text{thres, min}}$ due to the reduced amount of H_2 for V2B interactions and increased renewable electricity injected into the local power grid, the community and HVs have lower energy operating costs, but the office has an increased energy cost. According to the simulation results, when the $P_{V2B, \text{thres, min}}$ value increases from 20 to 70 kW, the energy operating costs of the community and HVs decrease from \$23344.0 to -\$689.8 and from \$14494.5 to \$4918.2 (H_2 cost), respectively; and the energy operating cost of the office increases from \$44096.7 to \$49651.4. Moreover, the fuel cell degradation cost is almost stable between \$10000 and \$11000. This is due to the fuel cell degradation is dominated by daily transportation (85 % or more of the total degradation). According to the comparison among the cases with different $P_{V2B, \text{thres, min}}$ values, Case 2 with the $P_{V2B, \text{thres, min}}$ value at around 40 kW might be an optimal condition for balancing the grid stability and energy operating costs of the inter-city energy migration network. Compared to the reference case, in the Case 2 with 40 kW $P_{V2B, \text{thres, min}}$, the maximum grid-export

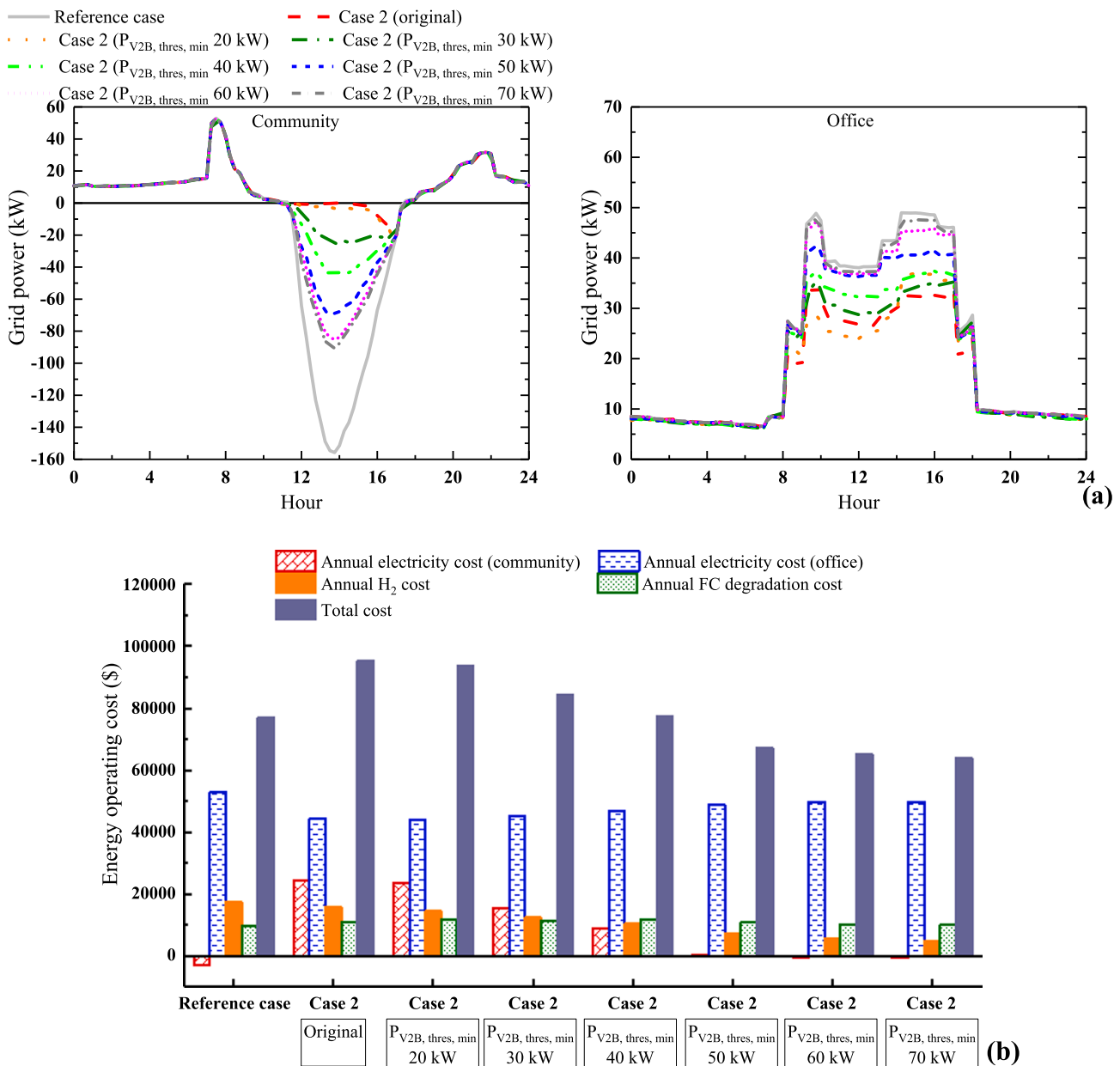


Fig. 11. The effects of peak-shaving grid-regulation strategy on (a) the grid powers and (b) the energy operating costs in Case 2.

power of the community is cut down by about 71 %, and the maximum grid-import power of the office is reduced by about 24 %. Meanwhile, the annual electricity cost of the office is \$46727.0, which is 11.5 % lower than that in the reference case. Meanwhile, the annual H₂ cost of the HVs is \$10327.4, which is 40.4 % lower than that in the reference case. Although the electricity cost of the community at \$8795.4 is higher than that in the reference case (-\$3076.2), it is 63.7 % lower than that in the original Case 2 without adopting the peak-shaving strategy. In other words, the peak-shaving strategy can effectively reduce the operating cost by shaving the peak power of the energy demand.

3.3.2. Load-shaping strategy

To show the effects of the load-shaping strategy on grid power and system operating cost, the $P_{V2B, \text{thres, min}}$ value is kept constant at 40 kW, and the $P_{V2B, \text{mag, max}}$ value is set from 10 to 30 kW, with an interval of 5 kW. Fig. 12(a) illustrates the mean hourly grid power with different

$P_{V2B, \text{mag, max}}$ values. The main finding is that compared to the peak-shaving strategy, the load-shaping strategy maintains similar grid stability and reduces the operating cost of the energy network. Specifically, when the $P_{V2B, \text{mag, max}}$ value increases from 10 to 30 kW, the grid-export power of the community decreases from 66.6 kW to 50.6 kW. The reason is due to the increased renewable-generated H₂ in V2B interactions and reduced renewable electricity exported to the grid. For example, when the $P_{V2B, \text{mag, max}}$ value is set at 10 kW, 847.1 kg H₂ is consumed by V2B interactions, and 9.3×10^4 kWh renewable electricity is exported to the local grid. When the $P_{V2B, \text{mag, max}}$ value is set at 30 kW, 1405.3 kg H₂ is consumed by V2B interactions, and 7.17×10^4 kWh renewable electricity of the community is exported to the local grid. Simultaneously, when the $P_{V2B, \text{mag, max}}$ value increases from 10 to 30 kW, the grid-import power of the office building decreases from 43.7 kW to 38.0 kW due to the increased amount of H₂ for V2B interactions. Moreover, as shown in Fig. 12(b), compared to the original Case 2, Case 2 with the

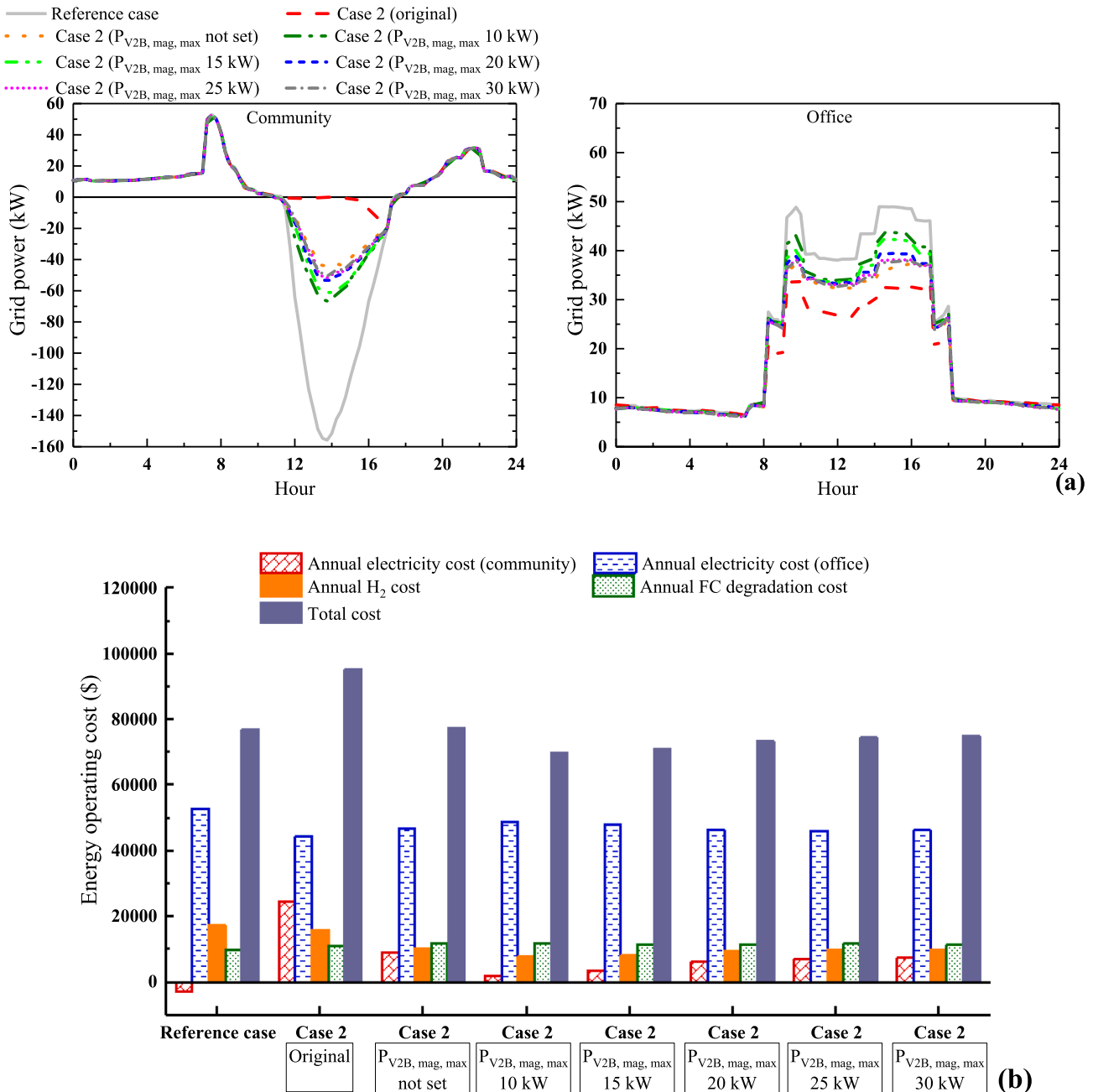


Fig. 12. The effects of load-shaping grid-regulation strategy on (a) the grid powers and (b) the energy operating costs in Case 2.

load-shaping strategy shows much higher economic benefits. For example, when the $P_{V2B, mag, max}$ value is 20 kW, the electricity cost of the community and the H₂ cost of the HVs are \$5980.4 and \$9211.4, which are 75.4 % and 41.6 % lower than those in the original Case 2, respectively. In other words, the load-shaping strategy can effectively reduce the operating cost of the community and the H₂ cost of the HVs, by prolonging the time-duration for V2B interaction. Meanwhile, compared to the original Case 2, there are slight increases in the electricity cost of the office building and the fuel cell degradation cost, only by 5.8 % and 5.5 %, respectively. However, due to the reduced grid-export electricity, the community with the load-shaping strategy still has a higher electricity cost than that in the reference case. This issue will be further discussed in Section 3.4.

3.4. Energy trading price thresholds for the economic feasibility of the inter-city energy migration network

As stated in Section 2.7, the proposed inter-city energy migration network is economically feasible only when the stakeholders have lower energy operating costs than that of the case when they are isolated from each other (the reference case). Here, Case 2 with a 40 kW $P_{V2B, thres, min}$ value and a 20 kW $P_{V2B, mag, max}$ value is adopted as an example to investigate the thresholds of energy trading price for the economic feasibility analysis. In this condition, 1.39×10^5 kWh renewable electricity of the community is exported to the H₂ system with the amount of

produced H₂ at 2404.1 kg. Meanwhile, 1051.4 and 1251.4 kg H₂ is consumed by daily transportation and V2B interactions, respectively, and 2.13×10^4 kWh electricity is provided by V2B interactions for covering the demand of the office building. The fuel cell degradation cost is \$11544.3, of which \$1708.6 is caused by V2B interactions. According to Section 2.7, the cost reduction in H₂-delivery of the H₂ station by the onsite-renewable-generated H₂ is \$10818.2, which is regarded as the maximum available payment of the community exporting renewable electricity to the H₂ station.

Fig. 13 shows the energy operating costs of the community, HVs, and office building with different energy trading prices. The energy trading price thresholds are determined when the corresponding costs are lower than those in the reference case. In terms of the community, the building-to-station electricity price threshold is identified as 0.07 \$/kWh (Fig. 13(a)). Namely, only when the price of the renewable electricity exported to the H₂ station is 0.07 \$/kWh or higher, the house owners will have a lower electricity cost by participating in the inter-city energy migration network than the case without participation in the energy network. It should be noted that the building-to-station electricity price at 0.08 \$/kWh surpasses the maximum available payment for the building-to-station energy trading. Thus, the building-to-station electricity price at 0.07 \$/kWh will be the optimal choice. For the HV cost (the sum of the H₂ cost and the fuel cell degradation cost), the price threshold of the onsite-renewable-generated H₂ is identified as 6.5 \$/kg (Fig. 13(b)). Namely, the HV owners will have lower operating costs

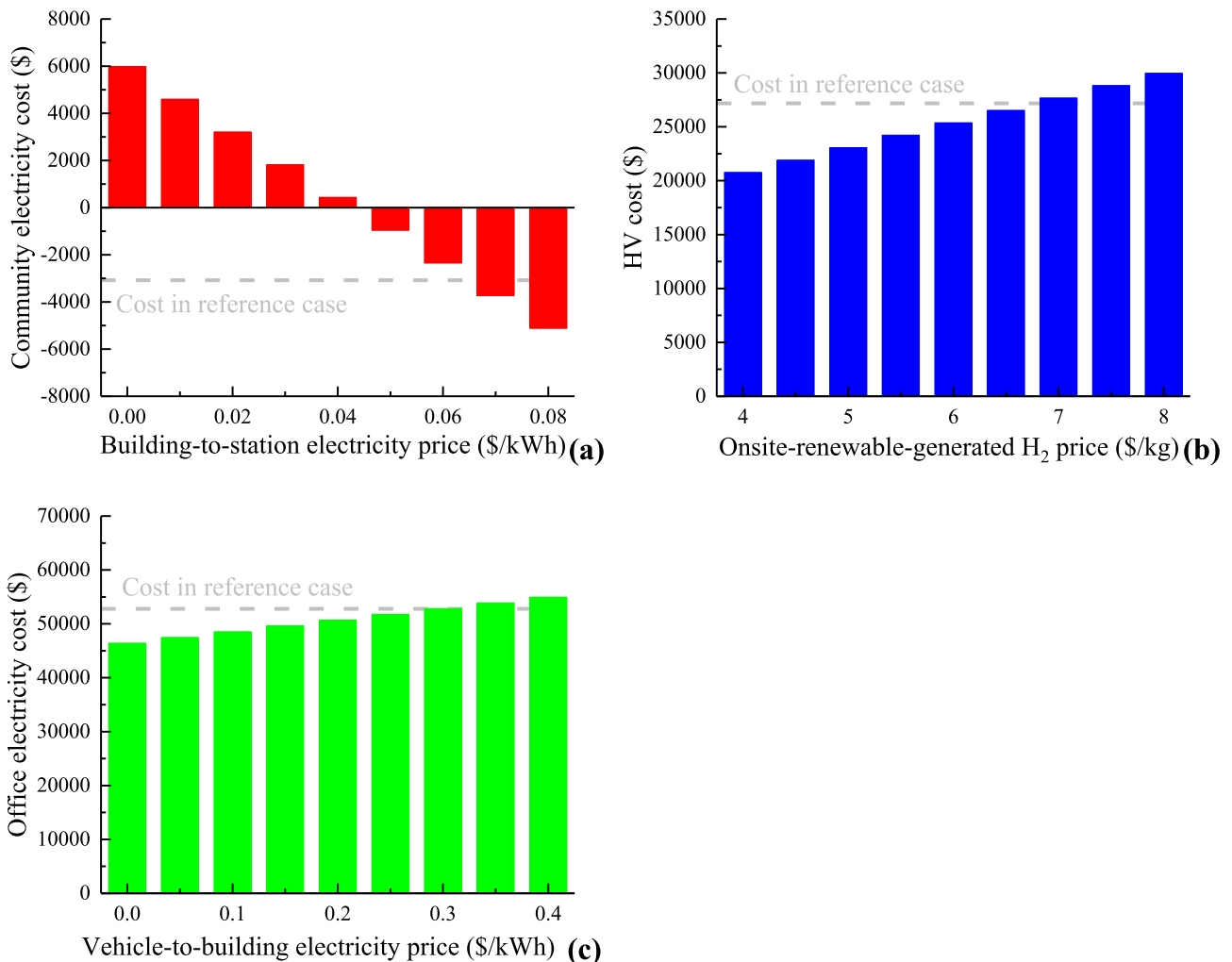


Fig. 13. The energy trading price thresholds for the economic feasibility of the proposed inter-city energy migration framework: (a) between the community and the H₂ station, (b) between the H₂ station and the HVs, and (c) between the HVs and the office building.

when the onsite-renewable-generated H₂ is lower than 6.5 \$/kg. Moreover, for the office building, the vehicle-to-building electricity price threshold is identified as 0.3 \$/kWh. Namely, only when the vehicle-to-building electricity price is lower than 0.3 \$/kWh, the office building owner will have a lower electricity cost than the case only relying on the local power grid. It should be noted that to guarantee the economic benefit of the office building owner, the vehicle-to-building electricity price threshold (0.3 \$/kWh) is at least 50 % higher than the grid-imported electricity price (see Table 2), indicating a potential promising extra payment (about \$6000 at most) for the HV owners to participate in the transportation-based energy migration framework.

4. Discussion

This study establishes an inter-city energy migration network, integrating a residential community, an office building, a H₂ station, HVs, local power grids, and local H₂ pipelines. The daily transportation of the HVs actualizes renewable energy migration from the energy prosumer (renewable abundant region, like the suburb residential community), to the energy consumer (demand-shortage region, like the city-center office building), which exerts promising benefits in spatiotemporal energy migration and regional energy balance, regional energy flexibility, grid stability, and energy operating costs for all involved stakeholders. Innovative grid-regulation strategies and energy trading strategies are proposed, to improve energy performance and economic feasibility. The findings of this study provide potential applications, as listed below:

- (1) The transportation-based inter-city energy migration provides a novel and low-cost approach to balance energy demands and renewable production between renewable-abundant and demand-shortage areas. Unlike conventional energy transmission approaches relying on pipelines and power grids, the transportation-based approach enhances inter-city building energy complementation and reduces grid burdens without massive infrastructure construction and capital investment costs. The inter-city energy migration network provides meaningful references and guidelines for developing H₂-based regional energy networks with high energy flexibility.
- (2) The proposed energy network, which is an inter-region hybrid electricity-H₂ energy system integrating buildings, renewable energy systems, HVs, a H₂ station, local power grids, and local H₂ pipelines, owns multiple energy interactions (electricity, H₂, and thermal energy) and advantages in energy efficiency, grid stability, regional energy balance, and cost efficiency. The proposed energy management strategies (including the grid-regulation solutions) of the inter-city energy migration network can achieve the trade-off among energy flexibility, grid stability, and energy costs of all stakeholders, providing the possibility to actualize regional energy balance, with win-win benefits for multilateral or trilateral benefits.
- (3) Unlike most previous studies that focus on the total energy cost, the energy trading strategies in this study consider the cost of every stakeholder and identify the critical threshold on energy trading price for economic feasibility, which sheds some light on promoting practical energy trading policies for low-carbon and cost-efficient regional energy networks.

Moreover, although this study is conducted with the background of California, the same problem, regional energy imbalance, exists in different regions with different climates and might be reduced through configuring the same or similar inter-city energy networks as the one proposed in this study, which integrates buildings, renewable energy systems, HVs, a H₂ station, local power grids, and local H₂ pipelines.

The limitations of this study should also be noted for enlightening future studies:

- (1) This study mainly demonstrates the benefits of transportation-based energy migration framework, and parametric analysis was conducted on grid-regulation strategies. Nonetheless, the impact of some design parameters on the techno-economic performance of the inter-city energy migration network, is ignored, such as the battery energy storage capacity, H₂ storage capacity, and so on. Based on the already developed platform and research results in this study, future studies will focus on the optimal design and synergistic operation between different energy storage systems.
- (2) Currently, the H₂ infrastructure in California is still under development and the aim is to support the demand of regional transportation. This study extends the application of H₂ infrastructure that, a H₂ station can also contribute to building energy flexibility, grid stability, and regional energy balance through deploying multiple energy interactions with its nearby buildings and vehicles. To further promote the regional H₂ energy application, the next step should be focused on the improvement of H₂ stations, in terms of covering regional energy demands, like domestic hot water, space heating, back-up electric power, H₂ gas for industries, oxygen supply, and even space cooling through absorption chillers.
- (3) Currently, California still has a high compensation price for grid feed-in tariff [30], which weakens the economic feasibility of the transportation-based energy migration framework and house owners' willingness to participate in the inter-city energy migration network. However, faced with the decreasing tendency of the grid feed-in tariff in the coming years [44], the economic feasibility of the inter-city energy migration network might be more promising and practical than the current status, which will be further explored in the future studies.
- (4) The techno-economic performance of the proposed inter-city energy migration network is investigated in the building context of California with a moderate climate. The performance of the network might be very different in other regions with different climates, transportation demands, energy infrastructures, energy prices, building types, and so on. These factors will be included in the future studies.
- (5) Based on the peer-to-peer energy trading [45] and optimization [46] in district community, future studies will explore the dynamic pricing model on peer-to-peer energy trading to maximize the economic benefits, together with advanced energy control strategies for lifecycle performance improvement [47]. Moreover, city-level analysis of solar photovoltaics will be assessed [48] with synergistic functions between hydrogen and power [49], in respect to power potential and price. Economic incentives need to be explored to promote multi-stakeholders to actively participate in the energy sharing network [50,51].

5. Conclusions

In this study, a transportation-based inter-city energy migration framework was proposed, integrating a residential community with rooftop PV systems and electrochemical batteries, an office building, HVs, a H₂ station connected to local H₂ pipelines, and local power grids. The techno-economic feasibility of the proposed energy migration framework has been studied, in terms of energy self-sufficiency, renewable self-use ratio, grid interaction, and energy operating costs. Innovative grid-regulation strategies (i.e., peak-shaving and load-shaping strategies) are proposed, to stabilize the grid power and reduce energy costs. In-depth analysis on different energy trading strategies and the critical thresholds on energy trading price are identified, to provide economic incentives and improve participation motivations for different stakeholders. Research results can provide frontier guidelines on the development of economically feasible regional building-vehicle energy networks with combined collaboration, efforts, and

participation from all stakeholders. The main conclusions of this study are summarized as follows:

- (1) Compared to the case with isolated buildings and vehicles (the reference case), the transportation-based energy migration framework can significantly enhance the grid independence of the office building and improve the renewable self-use ratio of the residential community. With the deployment of transportation-based energy migration framework, the energy self-sufficiency ratio of the office building can be improved from 0 % to 23.2 %, and the renewable self-use ratio of the residential community can be improved from 72.7 % to 98.6 %.
- (2) Compared to the reference case, the proposed transportation-based energy migration framework can mitigate the grid renewable congestion in the renewable-abundant region and the grid import pressure in the demand-shortage region. The energy migration framework can reduce the grid-export power of the residential community by up to 86.9 % (from 155.7 to 20.4 kW), and the grid-import power of the office by up to 29.4 % (from 49.0 to 34.6 kW).
- (3) By participating in the transportation-based energy migration framework, the energy operating costs of the office building and HVs (the H₂ cost and the fuel cell degradation cost) can be reduced by 16.4 % (from \$52791.3 to \$44154.7) and 1.7 % (from \$27172.5 to \$26707.4), respectively, whereas the grid-import cost of the community will increase from -\$3076.2 to \$24261.6 due to the reduced renewable electricity exported to the local power grid for compensating the grid-import cost.
- (4) The proposed grid-regulation strategies help balance the grid stability and the energy cost. When the lower threshold of V2B power is 40 kW, compared to the reference case, the community grid-export power is reduced by about 71.6 % (from 155.7 to 44.2 kW), and the office grid-import power is reduced by about 23.7 % (from 49.0 to 37.4 kW). Meanwhile, the annual electricity cost of the office and the annual H₂ cost of the HVs are \$46727.0 and \$10327.4, which are 11.5 % and 40.4 % lower than those in the reference case, respectively. The community grid-import cost is \$8795.4, which is 63.7 % lower than the case before deploying the grid-regulation strategy. Moreover, if the load-shaping strategy is added, the community grid-import cost can be further lowered to \$5980.4, which is 75.4 % lower than the case without the load-shaping strategy.
- (5) The critical thresholds on energy trading price are identified, to provide economic incentives and improve participation motivations from different stakeholders. Compared to the case with isolated buildings and vehicles, the transportation-based energy migration framework is economically feasible only when the price of the renewable electricity exported to the H₂ station for H₂ production is 0.07 \$/kWh for the community, the price of the onsite-renewable-generated H₂ is lower than 6.5 \$/kg for HV owners, and the vehicle-to-building electricity price is lower than 0.3 \$/kWh for the office building.

CRediT authorship contribution statement

Yingdong He: Conceptualization, Methodology, Investigation, Writing – original draft, Writing – review & editing. **Yuekuan Zhou:** Supervision, Project administration, Conceptualization, Methodology, Investigation, Writing – original draft, Writing – review & editing. **Jia Liu:** Investigation, Conceptualization, Methodology, Writing – review & editing. **Zhengxuan Liu:** Investigation, Writing – review & editing. **Guoqiang Zhang:** Investigation, Writing – original draft, Writing – review & editing.

Declaration of Competing Interest

The authors declare that they have no known competing financial interests or personal relationships that could have appeared to influence the work reported in this paper.

Acknowledgements

This study is supported by the funding of the Center for the Built Environment, University of California, Berkeley (Number: 59297 24003 44). This study is supported by the Hong Kong University of Science and Technology (Guangzhou) startup grant (G0101000059) and the Project of Hetao Shenzhen-Hong Kong Science and Technology Innovation Cooperation Zone (HZQB-KCZYB-2020083).

References

- [1] U.S. Energy Information Administration. U.S. energy facts explained, 2020. <https://www.eia.gov/energyexplained/us-energy-facts/>.
- [2] European Environmental Agency. Final energy consumption by sector and fuel in Europe; 2020. <https://www.eea.europa.eu/data-and-maps/indicators/final-energy-consumption-by-sector-10/assessment>.
- [3] He Y, Li N, Zhang H, et al. Air-conditioning use behaviors when elevated air movement is available. *Energy Build* 2020;110370.
- [4] He Y, Li N, Lu J, et al. Meeting thermal needs of occupants in shared space with an adjustable thermostat and local heating in winter: An experimental study. *Energy Build* 2021;236:110776.
- [5] Co T. Tesla Model S; 2021. <https://www.tesla.com/models>.
- [6] 2016 Toyota Mirai 4dr Sdn Features And Specs. https://www.caranddriver.com/toyota/mirai/specs/2016/toyota_mirai_toyota-mirai_2016.
- [7] Zhou Y, Cao S, Hensen JL, et al. Energy integration and interaction between buildings and vehicles: A state-of-the-art review. *Renew Sustain Energy Rev* 2019; 114:109337.
- [8] Zhou Y, Cao S, Kosonen R, et al. Multi-objective optimisation of an interactive buildings-vehicles energy sharing network with high energy flexibility using the Pareto archive NSGA-II algorithm. *Energy Convers Manage* 2020;218:113017.
- [9] Zhou Y, Cao S, Hensen JL, et al. Heuristic battery-protective strategy for energy management of an interactive renewables-buildings-vehicles energy sharing network with high energy flexibility. *Energy Convers Manage* 2020;214:112891.
- [10] Zhou Y, Cao S. Coordinated multi-criteria framework for cycling aging-based battery storage management strategies for positive building-vehicle system with renewable depreciation: Life-cycle based techno-economic feasibility study. *Energy Convers Manage* 2020;226:113473.
- [11] Qian F, Gao W, Yang Y, et al. Economic optimization and potential analysis of fuel cell vehicle-to-grid (FCV2G) system with large-scale buildings. *Energy Convers Manage* 2020;205:112463.
- [12] He Y, Zhou Y, Yuan J, et al. Transformation towards a carbon-neutral residential community with hydrogen economy and advanced energy management strategies. *Energy Convers Manage* 2021;249:114834.
- [13] He Y, Zhou Y, Wang Z, et al. Quantification on fuel cell degradation and techno-economic analysis of a hydrogen-based grid-interactive residential energy sharing network with fuel-cell-powered vehicles. *Appl Energy* 2021;303:117444.
- [14] Alavi F, Lee EP, van de Wouw N, et al. Fuel cell cars in a microgrid for synergies between hydrogen and electricity networks. *Appl Energy* 2017;192:296–304.
- [15] Sahu AV, Lee EHP, Lukszo Z. Exploring the potential of the vehicle-to-grid service in a sustainable smart city. In: 2018 IEEE 15th International Conference on Networking, Sensing and Control (ICNSC): IEEE; 2018. p. 1–6.
- [16] Felgenhauer MF, Pellow MA, Benson SM, et al. Evaluating co-benefits of battery and fuel cell vehicles in a community in California. *Energy* 2016;114:360–8.
- [17] Luo Y, Cheng N, Zhang S, et al. Comprehensive energy, economic, environmental assessment of a building integrated photovoltaic-thermoelectric system with battery storage for net zero energy building. *Building Simulation*: Springer; 2022. p. 1–19.
- [18] Luo Y, Zhang L, Liu Z, et al. Coupled thermal-electrical-optical analysis of a photovoltaic-blind integrated glazing façade. *Appl Energy* 2018;228:1870–86.
- [19] Google Map. California; 2021. <https://www.google.com/maps/place/%E5%8A%A0%E5%88%A9%E7%A6%8F%E5%B0%BC%E4%BA%9A/@37.1843034,-123.7975979,6z/data=!3m1!4b1!4m5!3m4!1s0x808fb9fe5f285e3d:0x8b5109a227086f5518m2!3d36.778261!4d-119.4179324>.
- [20] Sedy A. What solar incentives and rebates are available to California homeowners in 2021?; 2021 <https://www.solarreviews.com/blog/california-solar-incentives-calculator>.
- [21] Standard A. Standard 90.1-2019 “Energy Standard for Buildings Except Low-Rise Residential Buildings”. American Society of Heating, Refrigerating and Air-Conditioning Engineers, Inc Atlanta, GA, USA. 2019.
- [22] California Energy Commission. 2019 Energy Standards Lighting; 2019. <https://www.energy.ca.gov/programs-and-topics/programs/building-energy-efficiency-standards/online-resource-center/lighting>.
- [23] Engineering ToolBox. Hot Water Consumption per Occupant; 2003. https://www.engineeringtoolbox.com/hot-water-consumption-person-d_91.html.

- [24] CA 2007 Plumbing Code, Chapter 4; 2000. https://inspectapedia.com/plumbing/California_Plumbing_Code_Ch04.pdf.
- [25] Standard A. Standard 62.1-2019 "Ventilation for Acceptable Indoor Air Quality". American Society of Heating, Refrigerating and Air-Conditioning Engineers, Inc Atlanta, GA, USA. 2019.
- [26] Zhou W, Yang L, Cai Y, et al. Dynamic programming for new energy vehicles based on their work modes Part II: Fuel cell electric vehicles. *J Power Sources* 2018;407: 92–104.
- [27] Partnership CFC. Cost to refill; 202. <https://cafcp.org/content/cost-refill>.
- [28] International Renewable Energy Agency. Making Green Hydrogen a Cost-Competitive Climate Solution; 2020. <https://www.irena.org/newsroom/pressreleases/2020/Dec/Making-Green-Hydrogen-a-Cost-Competitive-Climate-Solution>.
- [29] Company PG&E. ELECTRIC SCHEDULE E-TOU-D; 2020. https://www.pge.com/tariffs/assets/pdf/tariffbook/ELEC_SCHEDULE_E-TOU-D.pdf.
- [30] Company PG&E. Understand Net Energy Metering and your bill; 2020. https://www.pge.com/en_US/residential/solar-and-vehicles/green-energy-incentives/solar-and-renewable-metering-and-billing/net-energy-metering-program-tracking/understand-net-energy-metering.page.
- [31] Company PG&E. Getting credit for surplus energy; 2020. https://www.pge.com/en_US/residential/solar-and-vehicles/green-energy-incentives/getting-credit-for-surplus-energy/getting-credit-for-surplus-energy.page.
- [32] Toyota Company. 2021 MIRAI; 2021. <https://www.toyota.com/mirai/>.
- [33] Alternative Fuels Data Center, U.S. Department of Energy. Hydrogen Laws and Incentives in California. <https://afdc.energy.gov/fuels/laws/HY?state=CA>.
- [34] Pei P, Chang Q, Tang T. A quick evaluating method for automotive fuel cell lifetime. *Int J Hydrogen Energy* 2008;33:3829–36.
- [35] Hou Y, Wan G, Jiang W, et al. Properties Analysis of Hydrogen Consumption Rate for a PEM Fuel Cell Engine. SAE Technical Paper; 2006.
- [36] Lohse-Busch H, Stutenberg K, Duoba M, et al. Technology assessment of a fuel cell vehicle: 2017 Toyota Mirai. Argonne National Lab.(ANL), Argonne, IL (United States); 2018.
- [37] A TRANSIENT SYSTEMS Simulation Program. Mechanical Engineering Department, UW Madison; 2017. <https://sel.me.wisc.edu/trnsys/>.
- [38] NeON® R ACe Solar Panels. [https://www.lg.com/us/business/download/resources/CT00002151/LG370-380A1C-V5_PRE_FinalVer_083019\[20190921_023718\].pdf](https://www.lg.com/us/business/download/resources/CT00002151/LG370-380A1C-V5_PRE_FinalVer_083019[20190921_023718].pdf).
- [39] Silverstein K. The World's Biggest Green Hydrogen Plant Is Planned For California. Its Prospects For Electric Power And Transportation?; 2020 <https://www.forbes.com/sites/kensilverstein/2020/05/26/the-worlds-biggest-green-hydrogen-plant-is-underway-in-california-its-prospects-for-electric-power-and-transportation/?sh=769872b02a96>.
- [40] U.S. Department of Energy. Costs of Storing and Transporting Hydrogen; 2014. <https://www.energy.gov/eere/fuelcells/downloads/costs-storing-and-transporting-hydrogen>.
- [41] Míguez J, López-González L, Sala J, et al. Review of compliance with EU-2010 targets on renewable energy in Galicia (Spain). *Renew Sustain Energy Rev* 2006; 10:225–47.
- [42] Tajitsu N, Shiraki M. Toyota plans to expand production, shrink cost of hydrogen fuel cell vehicles; 2018. <https://www.reuters.com/article/us-toyota-hydrogen-id-USKBN1KG0Y0>.
- [43] Wang D, Coignard J, Zeng T, et al. Quantifying electric vehicle battery degradation from driving vs. vehicle-to-grid services. *J Power Sources* 2016;332:193–203.
- [44] Pyrgou A, Kyllili A, Fokaidis PA. The future of the Feed-in Tariff (FiT) scheme in Europe: The case of photovoltaics. *Energy Policy* 2016;95:94–102.
- [45] Liu J, Yang H, Zhou Y. Peer-to-peer energy trading of net-zero energy communities with renewable energy systems integrating hydrogen vehicle storage. *Appl Energy* 2021. <https://doi.org/10.1016/j.apenergy.2021.117206>.
- [46] Liu J, Yang H, Zhou Y. Peer-to-peer trading optimizations on net-zero energy communities with energy storage of hydrogen and battery vehicles. *Appl Energy* 2021. <https://doi.org/10.1016/j.apenergy.2021.117578>.
- [47] Zhou Y, Cao S, Hensen JLM. An energy paradigm transition framework from negative towards positive district energy sharing networks—Battery cycling aging, advanced battery management strategies, flexible vehicles-to-buildings interactions, uncertainty and sensitivity analysis. *Appl Energy* 2021. <https://doi.org/10.1016/j.apenergy.2021.116606>.
- [48] Yan J, Yang Y, Campana PE, He J. City-level analysis of subsidy-free solar photovoltaic electricity price, profits and grid parity in China. *Nat Energy* 2019;4: 709–17.
- [49] Chen H, Song J, Zhao J. Synergies between power and hydrogen carriers using fuel-cell hybrid electrical vehicle and power-to-gas storage as new coupling points. *Energy Convers Manage* 2021;246:114670.
- [50] Zhou Y. Energy sharing and trading on a novel spatiotemporal energy network in Guangdong-Hong Kong-Macao Greater Bay Area. *Appl Energy* 2022;318:119131.
- [51] Zhou Y. Transition towards carbon-neutral districts based on storage techniques and spatiotemporal energy sharing with electrification and hydrogenation. *Renew Sustain Energy Rev* 2022;162:112444.